The multiple lncRNAs encoding *hsrω* gene is essential for oogenesis in *Drosophila*

Rima Saha and Subhash C. Lakhotia*

Cytogenetics Laboratory, Department of Zoology, Banaras Hindu University, Varanasi 221005, India

* Corresponding author

E-mail :

Rima Saha : rimasaha6@gmail.com

S. C. Lakhotia : lakhotia@bhu.ac.in

ORCID ID :

S. C. Lakhotia : orcid.org/0000-0003-1842-8411

Running Title : *hsrω* lncRNAs essential for *Drosophila* oogenesis

Abstract

To understand low viability and fecundity associated with perturbed levels of developmentally expressed and stress-inducible *hsrω* lncRNAs, we examined oogenesis in near-null *hsrω*^{66} homozygotes, and following targeted down- or up-regulation of *hsrω* transcripts in developing egg chambers. Short lifespan and poor fecundity, *hsrω*^{66} females showed fewer ovarioles, reduced Vasa and weak fusomes in early cysts, high apoptosis and poor actin nuclear-cage in mid-stage chambers, low Cut levels in late chambers and ovulation block. Effects of co-alterations in levels of *hsrω* transcripts, and oogenesis regulators like Notch, Cut, Caz/dFus and TBPH/TDP-43 on oogenesis were also examined. While altered *hsrω* transcript levels did not modulate defects following active Notch overexpression in follicle cells, they varyingly enhanced or suppressed defects due to targeted down- or up-regulation of Cut, Caz/dFus or TBPH/TDP-43. As expected of a gene producing multiple lncRNAs that interact with diverse regulatory molecules, simple linear causal inter-relations between oogenesis regulators and *hsrω* lncRNA levels were not evident. Ecdysone feeding to *hsrω*^{66} females or targeted expression of the *hsrω-RH* transcripts in *hsrω*^{66} egg chamber substantially restored normal oogenesis. Misexpression of *hsrω* lncRNAs thus adversely affects oogenesis through disruption of intra- and inter-organ signaling.

Keywords : Fecundity; Fusome; Ovulation block; Caz/dFus ; TBPH/TDP-43

Introduction

The *hsrω* gene is a developmentally active and cell stress inducible non-coding gene in *Drosophila melanogaster* (Lakhotia, 2011). This lncRNA gene produces 7 transcripts (www.flybase.org) using two transcription start sites and four termination sites and differential splicing of its single intron (Sahu et al., 2020). Earlier studies in our laboratory showed that the *hsrω* is highly expressed in the nurse and somatic follicle cells of ovary (Mutsuddi and Lakhotia, 1995) and absence of *hsrω* transcripts reduces fecundity of females (Lakhotia et al., 2012; Mallik and Lakhotia, 2011). To understand reasons for low fecundity of females with reduced *hsrω* transcripts, we examined oogenesis in $hsr\omega^{66}$ homozygous females. The $hsr\omega^{66}$ allele carries a 1.6 kb deletion that spans proximal part of the promoter and the first 9bp after the second (major) transcription start site (Johnson et al., 2011). Although the $hsr\omega^{66}$ mutation was claimed (Johnson et al., 2011) to completely abolish expression of the *hsrω* gene, and therefore, to be a null allele, subsequent studies in our lab (Ray et al., 2019a) revealed that the $hsr\omega^{66}$ allele is not a complete null but a near-null since traces of different *hsrω* transcripts are detectable in $hsr\omega^{66}$ homozygous individuals. The $hsr\omega^{66}$ homozygous individuals are 'unhealthy' (Johnson et al., 2011) with reduced fecundity (Mallik and Lakhotia, 2011). Present results showed that $hsr\omega^{66}$ females have short life span and poor fecundity because of poorly developed ovaries. Early-, mid- as well as late stages of oogenesis, including ovulation, are affected in these females. With a view to identify potential interactors through which the *hsrω* transcripts may act, genetic interaction studies involving targeted down- or up-regulation of Notch, Cut, Caz/dFus and TBPH/TDP-43 expression during oogenesis were carried. These revealed non-linear consequences of altered levels of one or more of these interactors, as expected of a gene producing multiple transcripts which interact with a wide variety of regulatory and other molecules in cell (Lakhotia, 2011; Ray et al., 2019a; Ray et al., 2019b; Singh and Lakhotia, 2015). Remarkably, providing ecdysone through food to $hsr\omega^{66}$ flies or targeted over-expression of the *hsrω-RH* transcript in ovarian follicle cells significantly restored the oogenesis defects associated with $hsr\omega^{66}$ homozygosity. The present results thus show that the *hsrω* lncRNAs are involved at several steps during the complex process of oogenesis and modulate the diverse intra- as well as inter-organ regulatory events through their multiple interactors to ensure its successful completion.

Materials and Methods

Fly strains and genotypes: All *Drosophila melanogaster* cultures were reared at $24^0 \pm 1^0$C on standard food containing agar, maize powder, yeast, and sugar. Following genotypes were used: 1) w^{1118} (as Control), 2) w^{1118}*;* $hsr\omega^{66}$ (Johnson et al., 2011), 3) w^{1118}*; UAS-hsrω-RNAi*^{3}, referred to here as *hsrωRNAi* (Mallik and Lakhotia, 2009), 4) w^{1118}*; EP93D/TM6B* (Sengupta and Lakhotia, 2006), 5) w^**; daGAL4/TM6B* (BDSC no. 55851), a ubiquitous GAL4 driver (Chaturvedi et al., 2016), 6) w^**; tjGAL4/CyO*, a follicle cell specific driver (Weaver et al., 2020) received from Dr. Pralay Majumder (Presidency University, India), 7) w^**; Act5CGAL4/CyO-GFP* (BDSC no. 4414), a ubiquitous driver (Hongay and Orr-Weaver, 2011) referred to here as *ActGAL4*, 8) w^{1118}*; UAS-hsrω-RH, carrying the UAS-hsrω-RH* transgene (Sahu et al., 2021) insertion on chromosome 3 (referred to here as *UAS-hsrωRH*), permitting targeted expression of the *hsrω-RH* transcript, 9) w^{1118}*; UAS-hsrωRH* $hsr\omega^{66}$*/TM6B*, 10) w^**; UAS-cutRNAi* (BDSC no. 33967), referred to here as *cutRNAi*, 11) w^**; UAS-cut/CyO* (Yadav et al., 2022), referred to here as *UAS-cut*, 12) *UAS-Notch*^{act,} for targeted expression of active Notch (Arya et al., 2015), 13) y^1 sc^{*1} v^1 sev^{21}*; +/+; UAS-cazRNAi* (dFus) (BDSC no. 34839), referred to here as *cazRNAi*, and 14) y^1 sc^{*1} v^1 sev^{21}*; UAS-TBPH-RNAi/CyO; +/+* (BDSC no. 39014 (Lanson et al., 2011)), referred to here as *TBPHRNAi*.

The obtain progeny of desired genotypes, appropriate genetic crosses were carried out.

Adult Life-span assay: Progeny flies of desired genotypes were collected immediately after eclosion and were grown in bottles/vials with food, supplemented with additional yeast for healthy growth. Three replicates of 20 females and males each of the desired genotypes were placed in food vials and transferred to fresh food vials at 3 days intervals till last of the $hsr\omega^{66}$ females survived (maximum 33 days); following the transfer of flies to fresh vial, dead flies in the previous vial were examined for their sex and genotype.

Fecundity assay: Flies of desired genotypes were collected soon after eclosion and grown in bottles with food, supplemented with additional yeast for healthy growth. Three replicates of 20 females and males each of the desired genotypes were placed in food vials. Flies were transferred into fresh food vials every day till day 14. Eggs laid in the previous vials during the one-day interval were counted to assay fecundity of females, which was expressed as eggs laid per female on a given day after eclosion.

20-hydroxy-ecdysone (20-HE) feeding: A stock solution (10mg/ml of ethanol) of 20-hydroxy-ecdysone (Cat no. H-5142 Sigma-Aldrich, India) was used to prepare ecdysone supplemented fly food with 20-HE at 0.05mM concentration. The w^{1118} and $hsr\omega^{66}$ flies were collected immediately after eclosion and transferred to fresh normal food vials, supplemented with additional yeast for healthy growth. On day 3 post-eclosion, 8-9 females and 1 male of the given genotype (w^{1118} or $hsr\omega^{66}$) were transferred to freshly prepared 20-HE supplemented food vials and allowed to feed for 115hr following which the 8day old flies were anaesthetized and dissected to remove ovaries for examination and immunostaining. Three biological replicates were carried out, and a total of 50 ovaries from 25 females of each genotype were examined.

Immunostaining of ovaries: Ovaries were removed from 6day old females of the desired genotypes, fixed, and processed for immunostaining as described earlier (Prasanth et al., 2000). The primary antibodies used were: 1) rat monoclonal anti-Vasa (1:10, DSHB), 2) mouse monoclonal anti-Alpha Spectrin (1:10, DSHB 3A9), 3) mouse monoclonal anti-Fasciclin III (1:20, DSHB 7G10), 4) mouse monoclonal anti-Cut (1:10, DSHB 2B10), 5) mouse monoclonal Anti-Hnt (1:10, DSHB), and 6) mouse monoclonal Anti-Caz/dFUS (1:10, 3F4, (Mallik et al., 2018)), provided by Dr. Moushami Mallik (Germany). Appropriate secondary antibodies conjugated with Alexa Flour 488 (1:200, Molecular Probes, USA) were used to detect the given primary antibody. Following the immunostaining, ovaries were counterstained with DAPI (4',6-diamidino-2-phenylindole dihydrochloride, Sigma-Aldrich, India; 1µg/ml), washed thrice in PBST for 20 minutes each, mounted in DABCO (1,4-diazabicyclo[2.2.2]octane), and observed by fluorescence and/or confocal microscopy. 20 ovaries were immunostained and examined for each antibody and genotype.

Phalloidin staining: To detect filamentous actin (F-actin), ovaries, fixed as above, were incubated in Phalloidin-TRITC (1:100, Sigma-Aldrich, India) for 12-16 hr at 4^0C. Subsequent washing and counterstaining steps were as for immunostaining.

Microscopy and documentation: Morphology of adult ovaries from flies of different genotypes were examined under a Nikon E800 microscope using 10X DIC optics. Confocal microscopy was carried out with Zeiss LSM 510 Meta laser scanning confocal microscope using Plan-Neofluor 5x (0.16 N.A.), Plan-Apo 10X (0.45 N.A.), Plan-Apo 20X (0.8 N.A.), or Plan-Apo 63X Oil (1.4 N.A.) with appropriate lasers and filters. Confocal images were analyzed with Zeiss LSM software. All images were assembled with Adobe Photoshop 7.0.

Results

Reduced life span and fecundity and interruption of oogenesis due to loss of *hsrω*-transcripts

Survival of w^{1118} (Control) and $hsr\omega^{66}$ homozygous female flies in different conditions was examined. The w^{1118} flies, which show normal lifespan and fecundity comparable to the wild type flies, were used as control in all experiments since all the other examined genotypes also carried w^{1118} or other *white eye* mutant allele.

As shown in Fig. 1A, all the $hsr\omega^{66}$ homozygous females, when kept with $hsr\omega^{66}$ homozygous males, did not survive beyond 33 days after emergence, although nearly 90% the w^{1118} females, maintained with w^{1118} males or with $hsr\omega^{66}$ homozygous males, survived till that day (Fig. 1A). Interestingly, keeping $hsr\omega^{66}$ homozygous virgin females with w^{1118} males further reduced their viability since none of these $hsr\omega^{66}$ females survived beyond 18 days after emergence (Fig. 1A).

Assay of fecundity of the $hsr\omega^{66}$ homozygous females, in terms of numbers of eggs laid by an individual female per day till 14 days after emergence, revealed that compared to w^{1118} females, the $hsr\omega^{66}$ females laid fewer eggs (Fig. 1B). Interestingly, keeping $hsr\omega^{66}$ virgin females with w^{1118} males further reduced the mean numbers of eggs laid/day but keeping $hsr\omega^{66}$ males with w^{1118} virgin females did not affect their egg-laying capacity (Fig. 1B). Besides the reduced numbers of eggs laid per day, the $hsr\omega^{66}$ females also showed a delayed onset of oviposition since no eggs were laid by them for the first 2 days of life.

To understand the delayed onset of oviposition and reduced fecundity of $hsr\omega^{66}$ homozygous females, their ovaries were examined on different days (20 ovaries of each genotype for each day) since eclosion (day 0). The ovaries were significantly smaller on day 0 in $hsr\omega^{66}$ homozygotes than in same age *white eye* females (Fig. 1C, D). Unlike the presence of stage 7-8 egg chambers in w^{1118} ovaries on day 0 (Fig. 1C), none of the same age $hsr\omega^{66}$ ovaries (Fig. 1D) had egg chambers beyond the stage 5-6. On day 1, $hsr\omega^{66}$ homozygous ovaries showed only a small increase in size (Fig. 1F) than the w^{1118} ovaries which showed developed mature follicles ready for ovulation (Fig. 1E). On day 3, the $hsr\omega^{66}$ females showed presence of some mature follicles (Fig. 1H), although the overall size of ovaries remained smaller than the day 3 w^{1118} ovaries (Fig. 1G). These observations agree with the above fecundity data that the $hsr\omega^{66}$ females start oviposition only on day 3 post-eclosion. Ovaries of the $hsr\omega^{66}$ homozygous females (Fig. 1I-L) on subsequent days (6th, and 8th) continued to show fewer ovarioles (Fig. 1J, and L) but a greater number of unovulated mature follicles, with shorter and abnormal dorsal appendages, (Fig. 2L) unlike in similar age w^{1118} ovaries (Fig. 1I, and K). Data for Mean number of ovariole number per ovary, and Mean number of mature follicles per ovary presented in Fig. 1M, and N, respectively (N=60 ovaries in each case) show that unlike in the *white eye* females (Fig. 1I, K), the mid- and late-stage egg chambers were very few in 6 days and older $hsr\omega^{66}$ homozygous females (Fig. 1J, L). The age-associated enhanced accumulation of mature follicles (multiple per ovariole, marked with black arrow) in the $hsr\omega^{66}$ homozygous females (Fig. 2J, L) suggests a block in ovulation (Deady et al., 2017; Knapp et al., 2019; Meiselman et al., 2018).

To understand the progression of oogenesis in $hsr\omega^{66}$ homozygous females, we next examined the germarium, mid-oogenesis and late-oogenesis stages using 6day old flies of different genotypes.

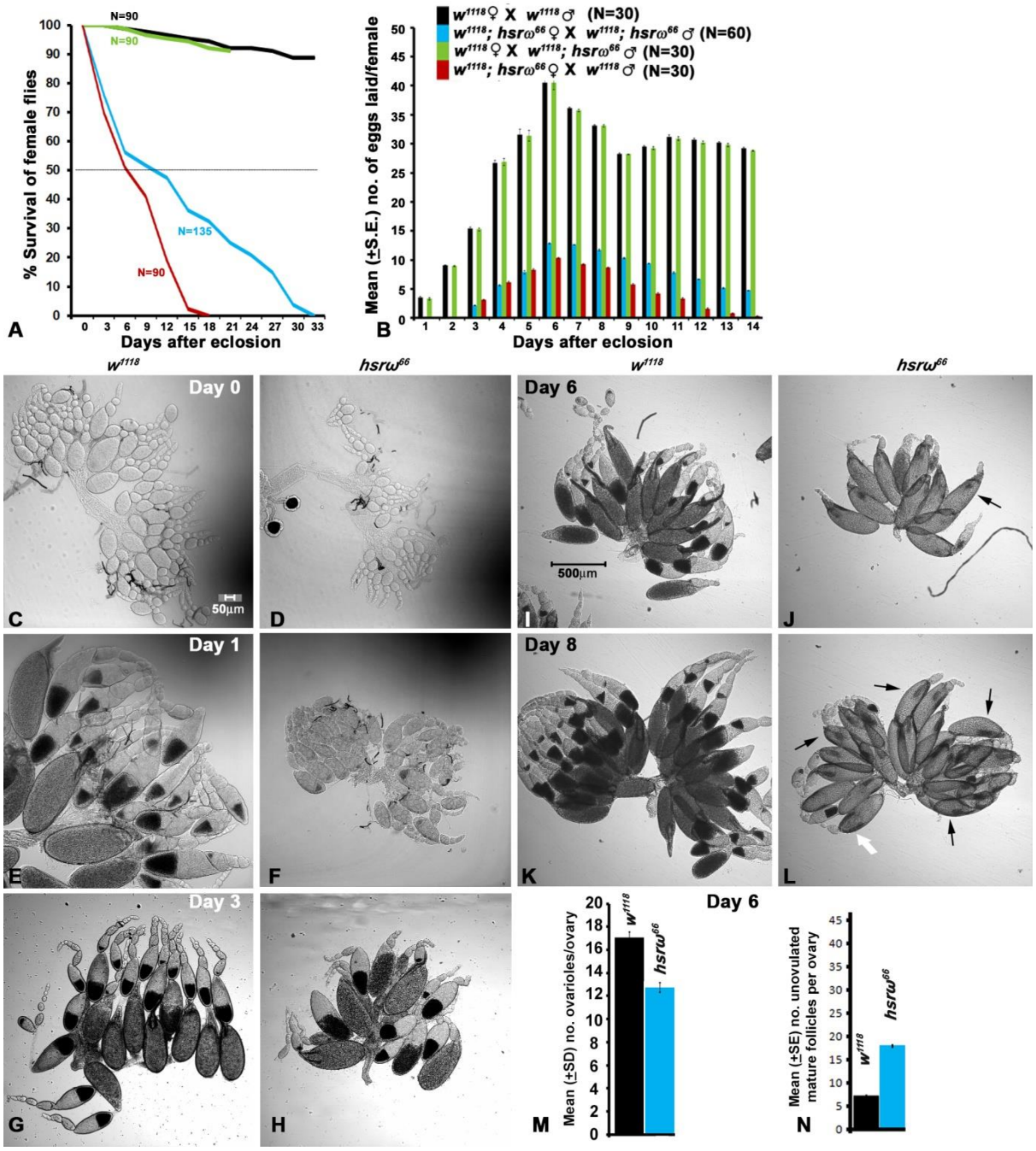

Fig. 1. Near absence of *hsrω* transcripts reduces lifespan and fecundity of *Drosophila* females, associated with poor ovarian growth, and ovulation block. (A) Lifespan of w^{1118} and $hsr\omega^{66}$ homozygous females crossed with males of different genotypes (noted on upper right corner in **B**); X-axis shows days after emergence while the Y-axis shows % survival of females on the given day. **(B)** Graphical presentation of the Mean (±S.E.) numbers of eggs laid (Y-axis) on different days after eclosion (X-axis) by w^{1118} and $hsr\omega^{66}$ homozygous females crossed with males of different genotypes (noted on upper right corner). N indicates the total numbers of flies examined (sum of 3 independent replicates) for each genotype. **(C-L)** Ovaries of w^{1118} (**C, E, G, I,** and **K**), and $hsr\omega^{66}$ homozygous (**D, F, H,** and **L**) females on day 0 (**C, D**), day 1 (**E, F**), day 3 (**G, H**), day 6 (**I, J**), and day 8 (**K, L**) after emergence; black arrows in **J** and **L** point to stacked mature follicles, while the white arrow in **L** point the abnormal dorsal appendages. (**M, N)** Histograms of the mean numbers (± S. D.) of ovarioles per ovary (Y-axis, **M**) and mean numbers (± S. D.) of mature follicles per ovary (Y-axis, **N**) on day 6 in w^{1118} and $hsr\omega^{66}$ homozygous females; N = 60 ovaries in each case. Scale bars in **C** and **I,** represent 50 µm and 500µm, respectively, and apply to **C-H** and **I-L,** respectively.

Germarium with poorly developed fusomes in *hsrω*^{66} homozygous ovaries

The germarium contains an elongated terminal filament composed of terminal filament cells (TF) at the anterior tip, which together with the cap cells (CC), and escort cells (EC) form the germ line stem cell (GSC) niche that surround and support the GSC maintenance (Eliazer and Buszczak, 2011; Kirilly and Xie, 2007). The total numbers of cap and terminal filament cells (N = 20 ovaries in each case) in w^{1118} (mean=13.08$\pm$0.03 S.E.) and *hsrω*^{66} homozygous (mean=12.99$\pm$0.02 S.E.) ovarioles were not significantly different. However, structure of the germarium appeared to be partly affected in the mutant females. The mid region (region 2b) of the germarium generally appears wider than its ends in wild type or w^{1118} (Fig. 2C) ovarioles, but in ~65% *hsrω*^{66} homozygotes, the region 2b of germarium appeared narrower and a little disorganized (Fig. 2D); only a few ovarioles (~8%) in w^{1118} females showed such abnormality.

Immunostaining for the germline marker RNA binding protein Vasa (Song et al., 2004; Yuan et al., 2012) revealed (Fig. 2E-H) that compared to w^{1118} ovarioles (Fig. 2E, G), the Vasa staining was detectably lower in the germarium region and the other early-stage egg chambers present in *hsrω*^{66} ovarioles in 6day old females (Fig. 3F, H). The mean numbers of the Vasa-positive GSCs residing nearest to the cap cells at the tip (marked with '#' in Fig. 2G, H) was 2.06 ($\pm$0.01 S.E.) in w^{1118} and 2.02 ($\pm$0.01 S.E.) in *hsrω*^{66} homozygous ovaries (Fig. 2G, and H, respectively), indicating that the *hsrω*^{66} mutation does not cause loss of GSCs although the Vasa protein level in them was reduced.

In *Drosophila*, a GSC differentiates into cystoblast (CB), which undergoes a series of four synchronous incomplete mitotic divisions to produce a cyst which generates the egg chamber or follicle (Greenbaum et al., 2011). After each round of mitosis, an endoplasmic reticulum derived membranous organelle, the fusome, grows along the cleavage furrow with remnants of the mitotic spindle; this connects all the cystocytes, which later produce the 15 nurse cell (NC) and a single oocyte within the cyst (Snapp et al., 2004). Fusomes, composed of four different components, including α- and ß-spectrin, are essential for the pattern and synchrony of these divisions during the egg chamber differentiation (Cox and Spradling, 2003; de Cuevas et al., 1996; Lighthouse et al., 2008; Lilly et al., 2000; Snapp et al., 2004). Immunostaining of w^{1118} and *hsrω*^{66} ovaries for α-spectrin (Fig. 2I-P) revealed that unlike the branched and robust fusomes in w^{1118} ovarioles (Fig. 2I and M), those in differentiating cysts of *hsrω*^{66} were significantly smaller and unbranched (Fig. 2J, N).

As noted earlier, the early- and mature follicles were present in the *hsrω*^{66} ovaries on day 6, the mid- and late-stages were very rare (Fig. 2K-L), which precluded a detailed comparison of the distribution of α-spectrin in w^{1118} and *hsrω*^{66} ovaries. In later w^{1118} and *hsrω*^{66} egg chambers, the overall distribution of α-spectrin was generally similar (Fig. 2K-L).

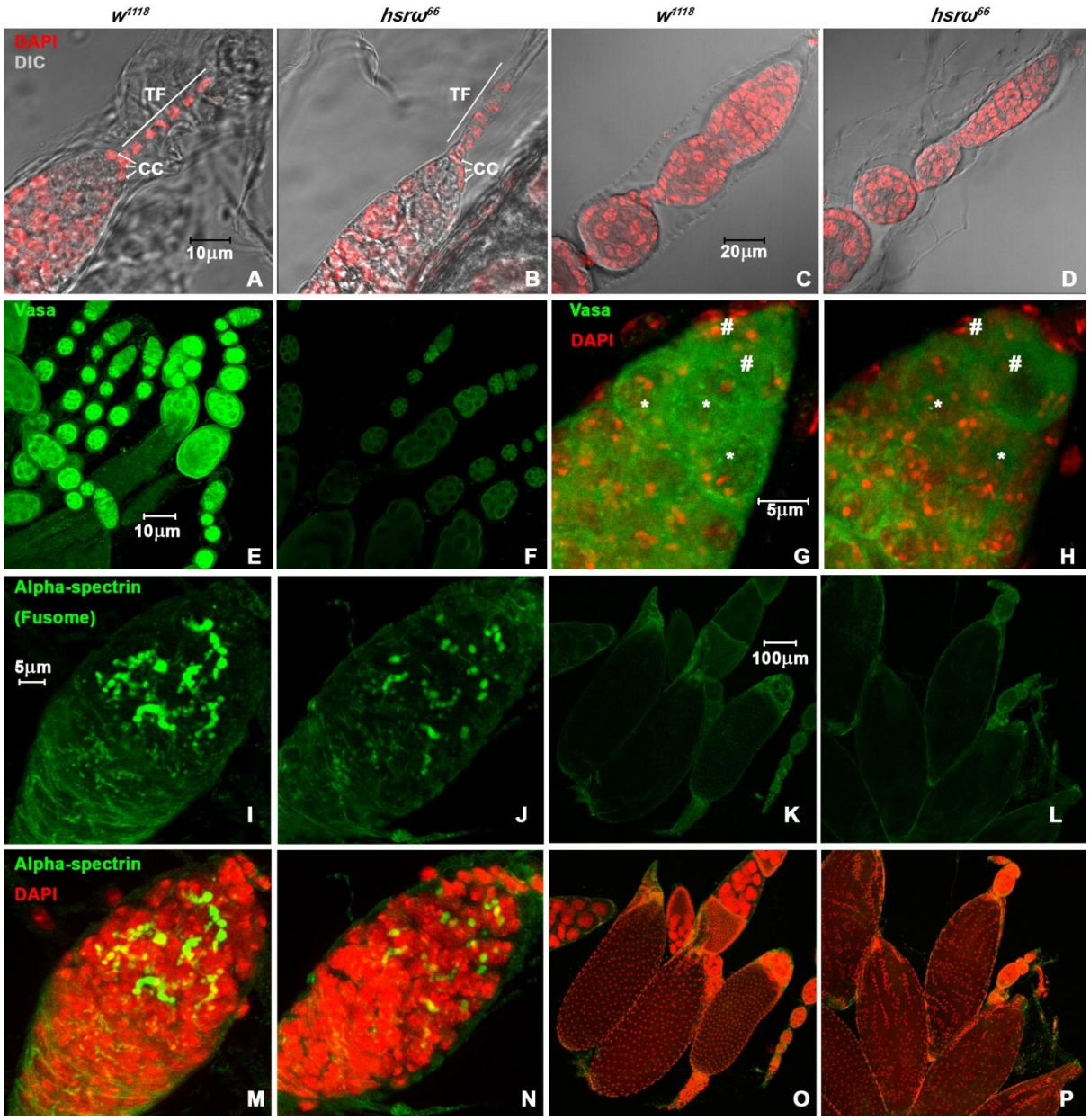

Fig. 2. Germarium shows reduced Vasa and poorly formed fusomes in *hsrω*^{66} ovaries. (A-D) Confocal projection images of DIC and DAPI (red) stained germarium regions of 6 days old *w*^{1118} (**A, C**) and *hsrω*^{66} (**B, D**) females; terminal filament cells (TF) and cap cells (CC) are marked with white line and white arrows, respectively. (**C-D**) DAPI stained germarium regions in 6day old *w*^{1118} (**C**) and *hsrω*^{66} (**D**). (**E-H**) Confocal projection images showing distribution of Vasa (green) in germarium region of 6day old *w*^{1118} (**E, G**) and *hsrω*^{66} (**F, H**) females; **G** and **H**, shown at higher magnification, also include DAPI (red) staining; GSCs and cystoblasts are marked with # and *, respectively. (**I-P**) Confocal projection images of α-spectrin (green) distribution in ovaries of *w*^{1118} (**I, K, M, and O**) and *hsrω*^{66} (**J, L, N, and P**) females; germarium containing α-spectrin (green) labelled fusomes are shown in **I** and **J**, while α-spectrin distribution in developing egg chambers and mature follicles is shown in (**K** and **L**); **M-P** show combined DAPI (red) and α-spectrin (green) staining. Scale bar in **A** = 10µm and applies to **A-B,** in **C** = 20µm and applies to **C-D**, in **E** = 10µm and applies to **E-F**, in **G** = 5µm and applies to **G-H**. Scale bar in **I** = 5 µm, and applies to **I, J, M,** and **N**; and in **K** = 100µm and applies to **K, L, O,** and **P**.

Fasciclin III and F-actin distribution affected *hsrω*^{66} ovarioles

Organization of the follicle cells in the germarium and developing egg chambers was examined through immunostaining for Fasciclin III (Fas III), which is a plasma membrane associated integral glycoprotein and is used as a follicle cell marker in ovarioles (Lee et al., 1997; Nystul and Spradling, 2010). The Fas III staining in the germarium region of *white eye* control and *hsrω*^{66} mutants (Fig. 3A-D) appeared generally similar except for a reduced level associated with the above noted narrower 2B region in *hsrω*^{66} mutants. Numbers and locations of different follicle cells in the few mid- and late-stage follicles present in *hsrω*^{66} ovaries appeared like those in *w*^{1118} ovaries. However, in the mature *hsrω*^{66} egg chambers (stage 13 and beyond), the follicle cell layer was highly disorganized as revealed by DAPI staining and Fas III marked cell membranes (compare Fig. 3E, I with B, F and J). Besides the disorganized distribution of follicle cells covering the maturing egg chambers, their nuclei also appeared slightly larger in *hsrω*^{66} than in similar age *w*^{1118} chambers (compare Fig. 3I and J).

Interestingly, unlike the Fas III rich small corpus luteum at the end of mature follicles in *w*^{1118} (Fig. 3K), the corpus lutea of the multiple unovulated mature egg chambers in *hsrω*^{66} ovaries fused with each other to make large Fas III positive bodies (Fig. 3L). The outer epithelial lining of proximal as well as distal parts of oviduct also showed less Fas III level in *hsrω*^{66} (Fig. 5N, and P) than in *w*^{1118} (Fig. 5M, and O).

The developing egg chambers in *hsrω*^{66} and *w*^{1118} ovaries were stained with Phalloidin (Fig. 3Q-V) to check the distribution of F-actin. The outer ovarian muscle layer in mid-stage *w*^{1118} (Fig. 3Q) and *hsrω*^{66} egg chambers (Fig. 3R) appeared comparable. However, compared to the robust deposition of F-actin in the nuclear cage in nurse cells of stage 10 *w*^{1118} egg chambers (Fig. 3S), the *hsrω*^{66} homozygous egg chambers showed very poorly formed nuclear cage (Fig. 3T). Mature *hsrω*^{66} egg chambers displayed significantly reduced F-actin in outer muscle layer also (Fig. 3U, V).

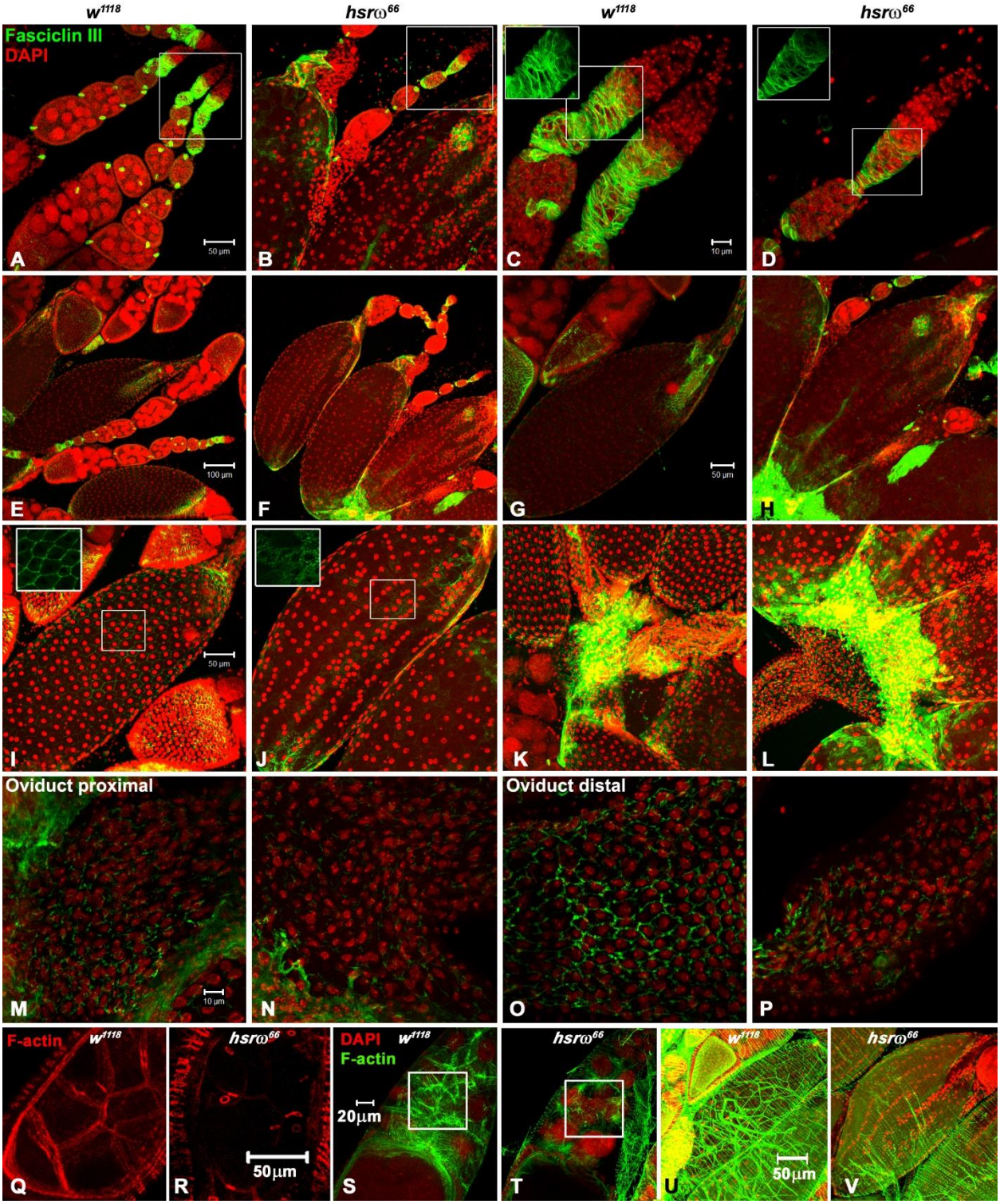

Fig. 3. Fasciclin III and F-actin show reduced levels in *hsrω*^{66} egg chambers. (A-P) Confocal projection images of combined DAPI (red) and Fas III (green) staining showing Fas III distribution in germarium to mid-stages (**A-D**), late stages (**E-H**) and mature follicles (**M-P**) in 6day old *w*^{1118} (**A, C, E, G, I, K, M,** and **O**) and *hsrω*^{66} (**B, D, F, H, J, L, N,** and **P**) females; (**C, D)** show higher magnification images of the boxed regions in germaria in **A** and **B**, respectively, with the insets in each showing only the Fas III staining of the boxed regions in each of the panels; insets in **I** and **J** show only Fas III staining to show follicle cell arrangement more distinctly in the two genotypes, **K** and **L**

show corpus luteum formed at the ends of the mature follicles; **M** and **N** show proximal parts of the Fas III stained (green) lateral oviduct, while **O** and **P** show distal parts of the lateral oviduct in w^{1118} and $hsr\omega^{66}$ flies. (**Q-V)** Confocal projection images of Phalloidin stained F-actin (red in **Q, R** and green in **S-V**) distribution in stage 8 (**Q, R**), stage 10 (**S, T**) and stage 13/14 (**U, V**) egg chambers in w^{1118} (**Q**, **S** and **U**) and $hsr\omega^{66}$ (**R**, **T** and **V**) females; DAPI staining (red) is also shown in **S-V**. Scale bar in **A** = 50µm and applies to **A-B,** in **C** = 10µm and applies to **C-D**, in **E** = 100µm and applies to **E-F**, in **G** = 50µm and applies to **G-H**, in **I** = 50µm and applies to **I-L**, in **M** = 10µm and applies to **M-P**, in B = 500µm and applies to **Q-R**, in **S** = 20µm and applies to **S-T** while that in **U** = 50µm and applies to **U-V**.

High frequency of apoptosis during mid-oogenesis in 6day old $hsr\omega^{66}$ females

The mid-oogenesis stage 8 is a check point for quality control of the developing egg chambers (Drummond-Barbosa and Spradling, 2001; Lebo and McCall, 2021; Pritchett and McCall, 2012). Since mid-stage egg chambers were remarkably rare in ovaries of 6day and older $hsr\omega^{66}$ flies (Fig. 1 to 3.3), we looked for signs of apoptosis as revealed by fragmented nuclei following DAPI staining. The w^{1118} ovarioles showed typical DAPI stained nurse and follicle cell nuclei in different stages of egg chambers (Fig. 4A) but egg chambers in $hsr\omega^{66}$ ovaries frequently displayed fragmented nuclei in nurse and/or follicle cells (Fig. 4B, white arrow), a characteristic feature of apoptosis. Since the number of ovarioles is not similar in the two genotypes, Mean % of stage 6-8 egg chambers per ovariole that showed apoptotic features was estimated in 60 ovaries of each genotype (Fig. 4E). The incidence of Mean % apoptotic 6-8 stage egg chambers per ovariole was significantly higher (13.11$\pm$1.01 S.E.) in $hsr\omega^{66}$ ovaries than in w^{1118} ovaries (3.62$\pm$0.45 S.E.).

In order to see if a targeted down-regulation of *hsrω* transcripts also affected mid-stage ovarian chambers, an ubiquitous *daGAL4* driver that expresses throughout oogenesis (Chaturvedi et al., 2016) was used to drive the *hsrωRNAi* transgene (Mallik and Lakhotia, 2011). The expected strong expression of *daGAL4* driver from mid-oogenesis stage 6-8 to mature follicles was confirmed by examining the EGFP expression in *daGAL4>UAS-EGFP* ovaries (Fig. 4C). Interestingly, a very high incidence of apoptotic egg chambers (Fig. 4D, white arrows) was observed in *daGAL4>hsrωRNAi* ovaries with Mean % mid-oogenesis apoptotic egg chambers per ovariole being 67.59 ($\pm$0.38 S.E., N=60; Fig. 6E).

Cut, but not Hindsight, expression is reduced during late-oogenesis in $hsr\omega^{66}$ ovarioles

The accumulation of large number of mature follicles at the posterior end of ovarian follicles, as seen in $hsr\omega^{66}$ ovaries (Fig. 2), is a characteristic feature of a block in ovulation (Deady et al., 2017; Knapp et al., 2019; Meiselman et al., 2018). Since Cut and Hindsight (Hnt) are known to play important roles in the ovulation process (Knapp et al., 2019), distribution of these two transcription factors in w^{1118} and $hsr\omega^{66}$ late stages egg chambers was examined by immunostaining (Fig. 4F-Q).

Cut is expressed transiently in the main body follicle cells during stages 10B-13 but disappears in stage 14 mature follicles (Knapp et al., 2019). Compared to the w^{1118} (Fig. 4F, H, and J), levels of Cut were low even in stage 10-13 $hsr\omega^{66}$ chambers (Fig. 4G, I, and K). During these stages, the highest level of Cut was observed in the anterior follicle cells of w^{1118} chambers, with the main body follicle cells being also Cut-positive (Fig. 4F and H); however, the levels of Cut in $hsr\omega^{66}$ stage 10-13 egg chambers, as assayed by immunostaining, were significantly lower in anterior follicle cells at all these stages, and nearly absent in body follicle cells at stages 10 and 13 (Fig. 4G, I, and K).

Hnt is not expressed in stage 11-13 follicle cells but its presence in the mature stage 14 follicles is essential for follicle rupture and ovulation competency (Knapp et al., 2019). As shown in (Fig. 4L-M), Hnt staining was relatively weak in follicle cells of early stages 7-10A $hsr\omega^{66}$ chambers (Fig.

4M) than in w^{1118} ovarioles (Fig. 4L), although as noted earlier, these mid-stage chambers were very few in the $hsr\omega^{66}$ ovaries. The stage 14 mature follicles in w^{1118} and $hsr\omega^{66}$ ovaries, however, showed more or less comparable Hnt levels, with higher levels in anterior (Fig. 4N-O) and posterior follicle cells (Fig. 4P-Q).

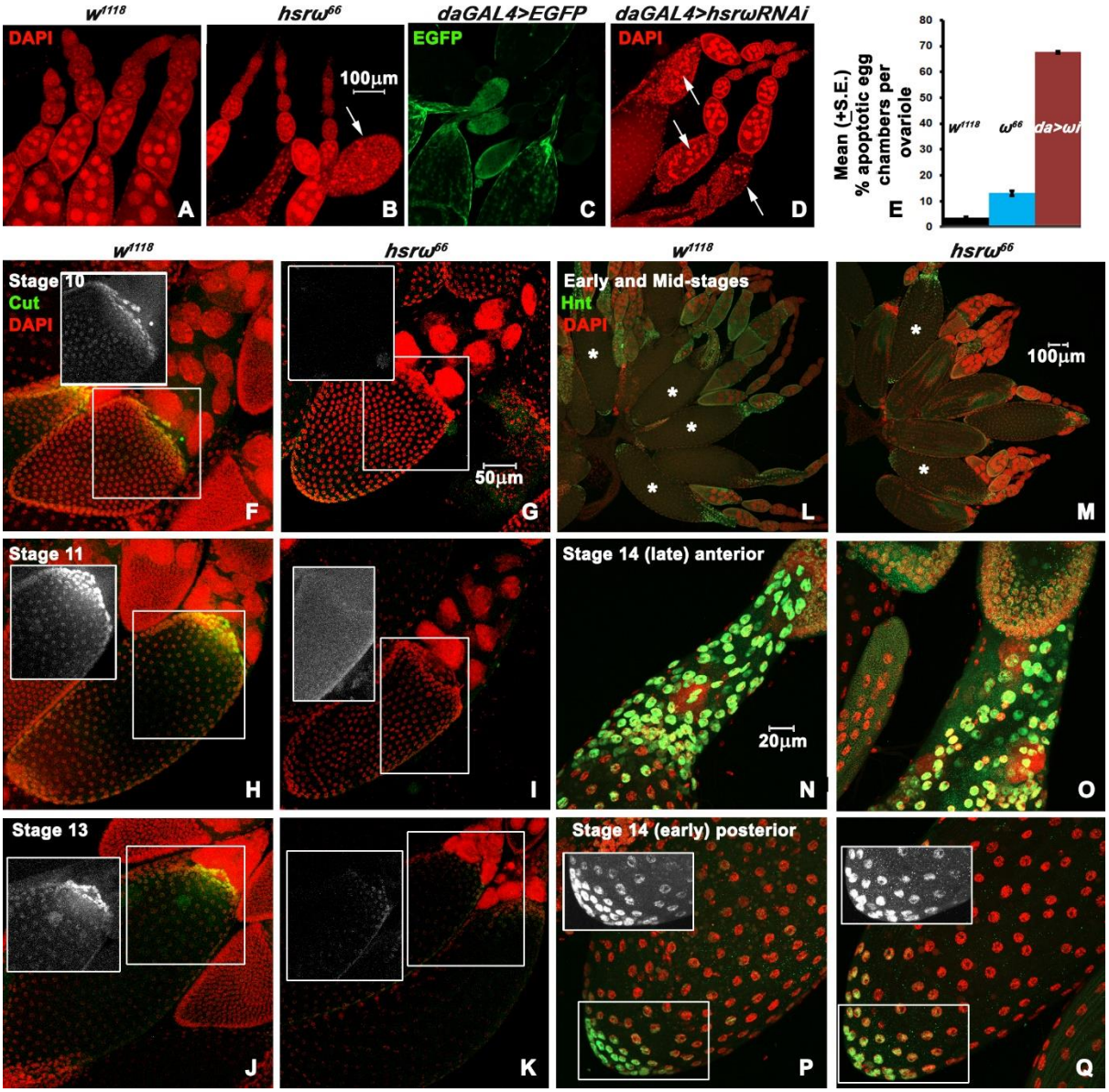

Fig. 4. Near absence or down-regulation of *hsrω* transcripts increases mid-stage apoptotic egg chambers and reduces Cut but not Hindsight (Hnt) during late oogenesis. (A, B) Confocal projection images of 6day old DAPI (red) stained ovarian follicles from w^{1118} (**A**) and $hsr\omega^{66}$ **(B)** females (N = 60 ovaries for each genotype). **(C)** Typical expression domain of *daGAL4* driver as revealed by expression of the *UAS-EGFP* (green) reporter. (**D**) Confocal projection image of DAPI (red) stained ovarian follicles from *daGAL4>UAS-hsrωRNAi*. White arrows in **B** and **D** indicate apoptotic egg chambers. (**E**) Histogram of Mean (±S.E.) % apoptotic egg chambers per ovariole (Y-axis) in ovaries of 6day old females (60 ovaries in each case) of different genotypes (X-axis). **(F-K)** Confocal projection images of 6day old Cut (green) and DAPI (red) stained stage 10 (**F** and **G**), 11 (**H** and **I**) and stage 13 (**J** and **K**) egg chambers from w^{1118} (**F, H, J**) and $hsr\omega^{66}$ **(G, I, K)** females; insets in **E-K** show only Cut staining (white) in the boxed region in the respective panels. **(L-Q)** Confocal projection images of 6day old Hnt (green) and DAPI (red) stained ovaries from w^{1118} (**L, N, P**) and $hsr\omega^{66}$ **(M, O, Q)** females showing full ovaries **(L, M)**, anterior part of mature stage

14 follicles **(N, O)** and posterior half of early stage 14 follicles **(P, Q)**; insets in **P**, and **Q** show only Hnt (white) staining in the boxed areas in the respective panels. Scale bar in **A** = 100µm and applies to A-D, in G = 50µm and applies to F-K, in M = 50µm and applies to L-M, and in **N** = 20µm and applies to **N-Q**.

Genetic interaction studies to identify potential interactors or targets of *hsrω* transcripts during oogenesis

In the next step, effects of GAL4-UAS driven alterations in expression of several known modulators of oogenesis in *Drosophila* in background of varying levels of *hsrω* were examined. In addition to the *hsrω*^{66}, we also used the *hsrωRNAi* transgene to down-regulate the *hsrω* transcripts and the *EP93D*, an *UAS*-carrying over-expression (*enhancer-promoter*) allele of *hsrω* (Mallik and Lakhotia, 2009; Sengupta and Lakhotia, 2006) to upregulate levels of these transcripts.

Since the above results indicated that follicle cells in the later stages of oogenesis are more affected in *hsrω*^{66} ovaries, we used a follicle cell specific *tjGAL4* driver (Weaver et al., 2020) to modulate expression of some known regulators of oogenesis through their roles in follicle cells. The follicle cell specific expression of this driver was confirmed by monitoring the GFP expression in *tjGAL4>UAS-EGFP* ovaries (Fig. 5A-C). In some experiments described later, we also used ubiquitous *ActGAL4* (Hongay and Orr-Weaver, 2011), whose expression in ovarioles was confirmed by monitoring the GFP expression in *ActGAL4>UAS-EGFP* ovaries (Fig. 5D).

Efficiency of the *tjGAL4* driven *RNAi* system was further confirmed by examining immunostaining for the Caz/dFus (fly homolog of the human FUS protein) protein in *tjGAL4>UAS-cazRNAi* ovaries since as described later (Fig. 7), the Caz protein shows high expression in follicle cells during normal oogenesis. As expected, Caz staining was absent in follicle cells in *tjGAL4>UAS-cazRNAi* early-, mid- and late-stage egg chambers (Fig. 5E, F). Surprisingly, however, following its absence in follicle cells in the mid-stage egg chambers, Caz expression was found to be upregulated in nurse cells (Fig. 5E, F).

We examined effects of *tj-GAL4* driven down- (*tjGAL4>hsrωRNAi*) or up-regulation (*tjGAL4>EP93D*) of *hsrω* transcripts in follicle cells. Interestingly, the *tj-GAL4* driven down- (*tjGAL4>hsrωRNAi*) or up-regulation (*tjGAL4>EP93D*) of *hsrω* transcripts in follicle cells caused ovarian defects similar in several respects to those in the *hsrω*^{66} ovaries since the 6day old females of either genotype showed ovulation block and enhanced apoptosis of mid-stage chambers. Consequently, in both cases the numbers of unovulated mature follicles were high while the developing egg chambers in each ovariole were very rare (Fig. 5G, H; Table 1). The *tjGAL4>EP93D* ovaries appeared more affected than *tjGAL4>hsrωRNAi* since the former ovaries were often asymmetric because of fewer/smaller ovarioles in one of the ovaries (Fig. 5H) and displayed greater ovulation block with stacks of three unovulated eggs being frequent.

Notch (N)

The interacting Notch and Cut are major regulators of oogenesis and ovulation in *Drosophila* (Deady et al., 2017; Jackson and Blochlinger, 1997; Sun and Deng, 2005). Therefore, these two genes were checked for their interactions with *hsrω*. Notch down-regulates *cut* in follicle cells for their switching from mitotic to endo-cycles and differentiation (Sun and Deng, 2005). With a view to examine if Notch signaling is affected in follicle cells in ovaries mis-expressing *hsrω*, active Notch (*UAS-N*^{Act}) was over-expressed by driving with *tjGAL4* in ovaries with varying levels of *hsrω* transcripts. Expression of *UAS-Notch*^{Act} under the *tjGAL4* driver resulted in complete absence of egg chambers beyond stage 9 (Fig. 5I) because of high frequency of late-stage apoptosis (Fig. 5M). The *tjGAL4>UAS-N*^{Act}*/hsrω*^{66} (heterozygous for *hsrω*^{66}) or *tjGAL4>UAS-N*^{Act}*/hsrωRNAi* or

tjGAL4>UAS-N^{Act}/EP93D ovaries did not modify the *tjGAL4>UAS-N^{Act}* ovarian phenotype since in all these cases, ovaries in 6day old females did not show any egg chamber beyond stage 9 (Fig. 5J-P). As expected, none of these females laid any eggs.

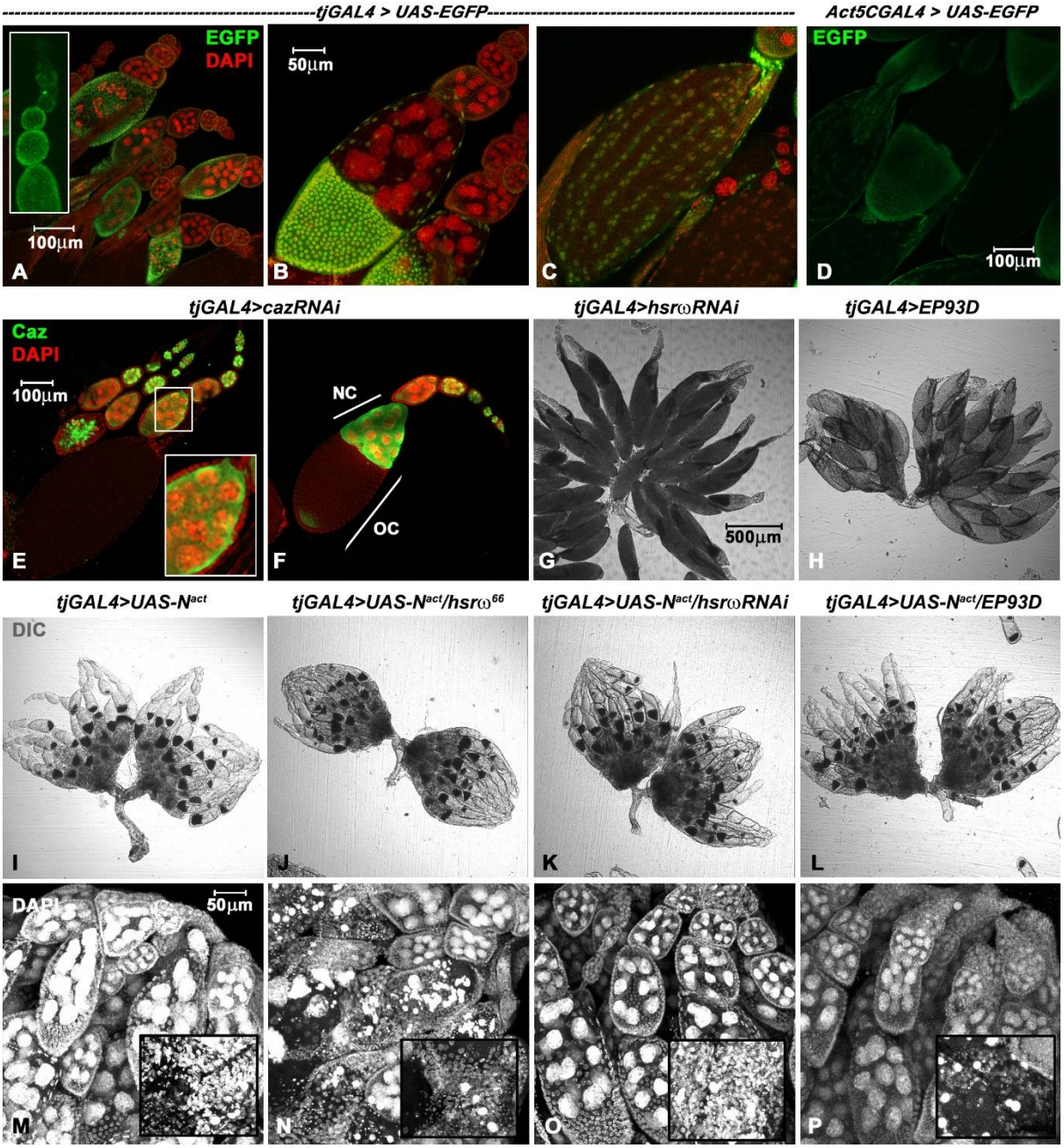

Fig. 5. The follicle-cell specific *tjGAL4* driven mis-expression of *N* in follicle cells completely disrupts later stages of oogenesis irrespective of levels of *hsrω* transcripts. (A-C) Confocal projection images of GFP expression (green) at different stages of oogenesis in 6 day old *tjGAL4>UAS-EGFP* ovaries counterstained with DAPI (red); the inset in **A** shows only GFP expression in *tjGAL4>UAS-EGFP* germarial region and early egg chambers. (**D**) *ActGAL4>EGFP* expression (green) during mid-stages of oogenesis. (**E, F**) Confocal projection images of Caz expression (green) in 6day old *tjGAL4>cazRNAi* ovarioles counterstained with DAPI (red); a stage 8 egg chamber is shown inset in **E**; **F** shows a stage 12 egg chamber with nurse cells (NC) and oocyte (OC) marked. **(G-L)** DIC images of *tjGAL4>N^{Act}* (**I**), *tjGAL4>UAS-N^{Act}/hsrω^{66}* (heterozygous for *hsrω^{66,}* **J**), *tjGAL4>UAS-N^{Act}/hsrωRNAi* (**K**) and *tjGAL4>UAS-N^{Act}/EP93D* (**L**) ovaries from 6day old flies. **(M-))** DAPI-stained (white) magnification images parts of ovarioles in **I-**

L, respectively; insets in these panels show apoptosis in >stage 9 chambers. Scale bar in **A** = 100µm; in **B** =50 µm and applies to **B-C**, in **E** = 100µm and applies to **E-F**, in **G** = 500µm and applies to **G-L**, in **M** = 50µm and applies to **M-P**.

Cut

Expression of *cut* is restricted to somatic follicle cells and maintains germline cyst integrity (Jackson and Blochlinger, 1997). Cut also regulates mitotic cycles in the follicle cells during early oogenesis (Sun and Deng, 2005) and through its dose-sensitive interaction with *cappuccino* influences soma and germline interactions during oogenesis (Jackson and Berg, 1999). Cut must be rapidly downregulated in stage 14 mature follicles to allow its ovulation (Knapp et al., 2019). Expression of *tjGAL4>cutRNAi* in wild type *hsrω* background did not affect the ovary size or the numbers of ovarioles (Fig. 6A, E) and the early stages of egg chambers. However, from the mid-oogenesis onwards the antero-posterior (A-P) axis of egg chambers was significantly reduced resulting in smaller and rounded mature follicles with aberrant dorsal appendages (insets in Fig. 6A); these ovaries also displayed significant apoptosis after mid-stage egg chambers (Fig. 6E), disrupted follicle cell arrangement (inset in Fig. 6E) and ovulation block (Fig. 6A). Phenotypes of *tjGAL4>cutRNAi/hsrω*^{66} (heterozygous for *hsrω*^{66}) and *tjGAL4>cutRNAi/hsrωRNAi* (Fig. 6B, C, F, G) were generally like those seen in *tjGAL4>cutRNAi* ovaries but with a more pronounced absence of mid-stage chambers between the string of early- and late-stage follicles in ovarioles, especially in *tjGAL4>cutRNAi/hsrω*^{66}. It is interesting that even a single copy of *hsrω*^{66} in these trans-heterozygotes had some enhancing effect on the *tjGAL4>cutRNAi* phenotype. Follicle cell layer covering the mature, but roundish follicles was disorganized in all the three genotypes (insets in Fig. 6E-G). Females of all the three genotypes laid roundish eggs which developed into viable larvae (data not presented). Interestingly, ovaries in *tjGAL4>cutRNAi/EP93D* appeared significantly better since mid-stage chambers were more frequent than in the previous three genotypes and the organization of follicle cell layer and length of mature follicles were nearly like those in wild type; the ovulation block was also substantially rescued (Fig. 6D, H). Shape of the eggs laid by *tjGAL4>cutRNAi/EP93D* females was nearly like that in wild type (not shown).

Over-expression of *cut* in *tjGAL4>UAS-cut* ovaries resulted in grossly disorganized progression of oogenesis, since in 6day old female ovaries, the germarium region and developing egg chambers lost their characteristic appearance so that no mature follicles were present in these ovaries (Fig. 6I, M); yolk was abnormally located (Fig. 6.9I). Over expression of Cut under *tjGAL4* driver in *hsrω*^{66} or *hsrωRNAi* background (*tjGAL4>UAS-cut; +/hsrω*^{66} and *tjGAL4*>UAS-*cut; +/hsrωRNAi*) also resulted in disorganized ovarioles (Fig. 6J, K, N, O), with the *tjGAL4*>UAS-*cut* phenotype dominating. Apparently, effect of ectopic over-expression of Cut in follicle cells is epistatic to consequences of reduced levels of *hsrω* transcripts. Surprisingly, co-over-expression of Cut as well as *hsrω* transcripts under the *tjGAL4* driver (*tjGAL4>UAS-cut; +/EP93D*) significantly improved the ovarian organization till the mid-stage egg chambers although the late-stage chambers showed high frequency of apoptosis (Fig. 6L, P). None of the females with down- or up-regulated Cut expression under the *tjGAL4* driver, without or with altered levels of *hsrω* transcripts, but laid eggs.

Together these results further confirm interaction between *cut* and *hsrω* as also indicated by the earlier noted (Fig. 4) reduced levels of Cut in *hsrω*^{66} ovaries. Intriguingly, however, down- as well as up-regulation of Cut nearly completely or partially mitigated by co-expression of *EP93D* which enhances the levels of *hsrω* transcripts.

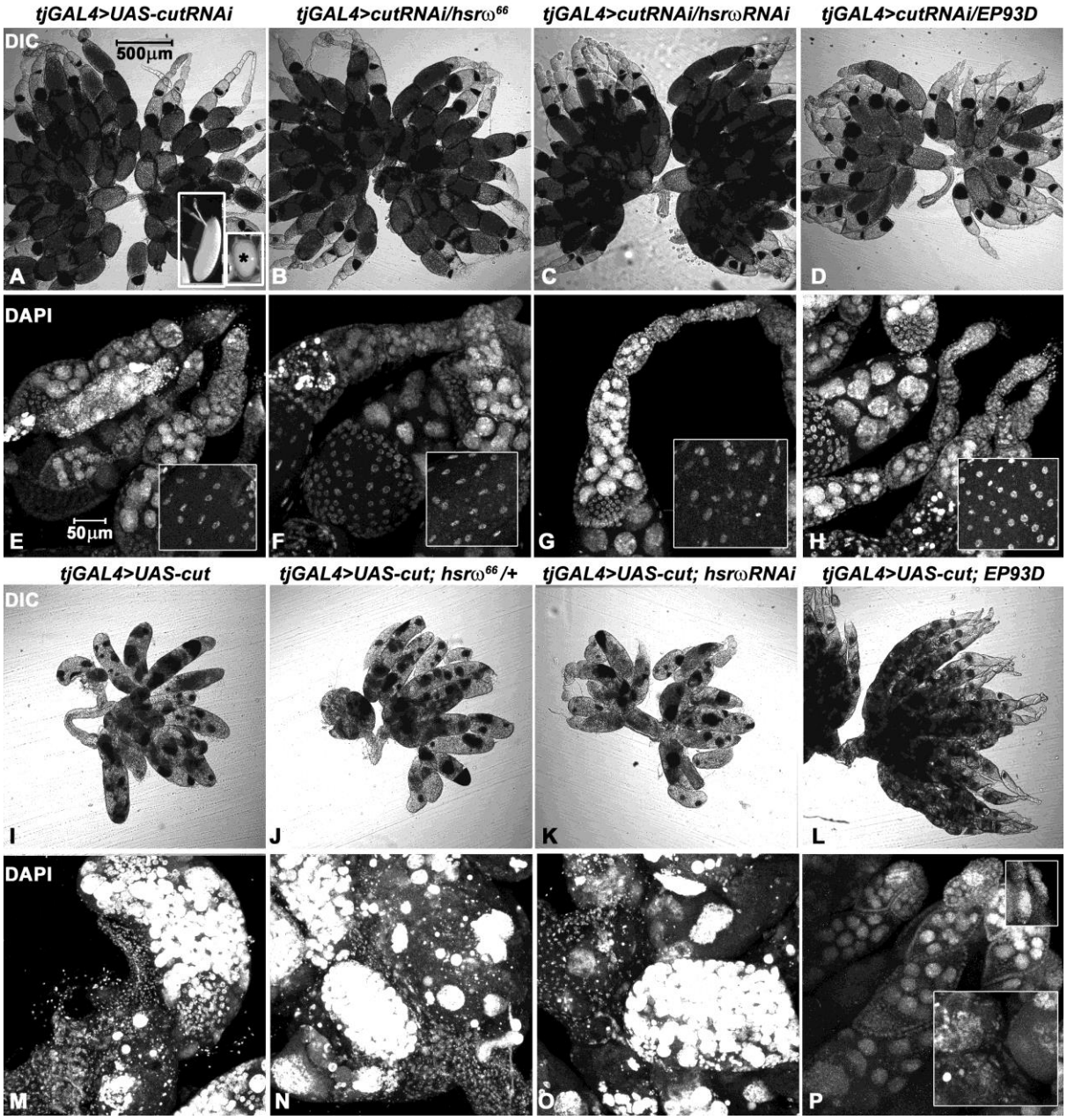

Fig. 6. Over-expression of *hsrω* fully or partially rescues effects of down- or up-regulation of Cut in follicle cells of ovaries. (A-D) DIC images of *tjGAL4>cutRNAi* (**A**), *tjGAL4>cutRNAi/hsrω*^{66} (**B**), *tjGAL4>cutRNAi/hsrωRNAi* (**C**) and *tjGAL4>cutRNAi/EP93D* (**D**) ovaries; insets in A show the normal elongated wild type and rounded and smaller *tjGAL4>cutRNAi* (marked *) eggs. **(E-H)** DAPI-stained higher magnification images of ovarioles from the ovaries shown in **A-D**, respectively; insets in **E-H** show patterns of the follicle cells in mature follicles in each case. **(I-L)** DIC images of *tjGAL4>UAS-cut* (**I**), *tjGAL4*>UAS-*cut hsrω*^{66}/+ (**J**), *tjGAL4*>UAS-*cut hsrωRNAi* (**K**), and *tjGAL4*>UAS-*cut EP93D* (**L**) ovaries. **(M-P)** DAPI-stained higher magnification images of the ovaries in **I-L**, respectively; inset on upper right corner of **P** shows the germarium region while that at lower right side shows apoptotic chambers close to lateral oviduct. Scale bar in **A** = 500µm and applies to **A-D**, and **I-L**; in **E** =50 µm and applies to **E-H**, and **M-P**.

We next looked for some of the known interactors of *hsrω* to understand how *hsrω*-transcripts may affect oogenesis and ovulation. Although several hnRNPs that interact with *hsrω* have been reported to have essential functions like fecundity regulation (Singh and Lakhotia, 2012), and GSC

self-renewal (Casale et al., 2019; Finger et al., 2022), none of these are specifically found to be required for ovulation. Therefore, we selected two recently known interactors namely *caz*/dFus and TBPH/TDP-43 (Lanson et al., 2011; Lo Piccolo et al., 2018; Lo Piccolo et al., 2017; Lo Piccolo and Yamaguchi, 2017) to examine their roles in oogenesis, if any.

Caz

Recently, Caz/dFUS (*Drosophila* homolog of human FUS) hnRNP has been shown to physically interact with the *hsrω-n* RNA (Lo Piccolo et al., 2017). Since expression of Caz during normal oogenesis in wild type or w^{1118} ovaries has not yet been described, we first examined expression patterns of Caz in w^{1118} and $hsr\omega^{66}$ ovaries by immunostaining (Fig. 7A-D). As shown in Fig. 7, Caz was expressed from germarium to mature follicles in w^{1118} ovaries, (Fig. 7A, C). In the germaria and early egg chambers, Caz was present in germline as well as somatic cells (Fig. 7E). During mid-oogenesis, however, Caz was seen abundantly in all the follicle cells but not in the germline nurse cells and oocyte (Fig. 7F, and K). The ovarian sheath cells showed strong presence of Caz (white arrows in Fig. 7F, Q-T). In stage 14 mature follicles, the posterior follicle cells, which undergo trimming to allow ovulation of the follicle, expressed Caz at a higher level than the body follicle cells (Fig. 7G). At the anterior end of mature follicles, the corpus luteum showed high levels of Caz (Fig. 7H). As known in other tissues (Lanson et al., 2011; Lo Piccolo et al., 2017; Lo Piccolo and Yamaguchi, 2017), Caz protein was nuclear in all the ovarian cell types that expressed it.

The Caz expression in the $hsr\omega^{66}$ germarium region (Fig. 7J) was like that in w^{1118} (Fig. 7I) although the staining intensity appeared weaker in all cell types. During mid-oogenesis, the follicle cells showed presence of Caz in both the genotypes (Fig. 7K-L). Caz was absent in nurse cells in both the genotypes as clearly visible in optical sections of w^{1118} (Fig. 7K) and $hsr\omega^{66}$ (Fig. 7L) mid-stage chambers. Unlike the forward movement and consequent sparse distribution of anterior follicle cells in early stage 14 follicles in w^{1118} ovarioles (Fig. 7M, Q), those in similar stage $hsr\omega^{66}$ chambers remained more closely spaced at base of the anterior end (Fig. 7N, R); however, the Caz staining patterns in these cells in the two genotypes were generally comparable. At late stage 14, the follicle cells at the anterior end showed much stronger Caz expression in w^{1118} (Fig. 7O, and S) than in the $hsr\omega^{66}$ (Fig. 7P, and T).

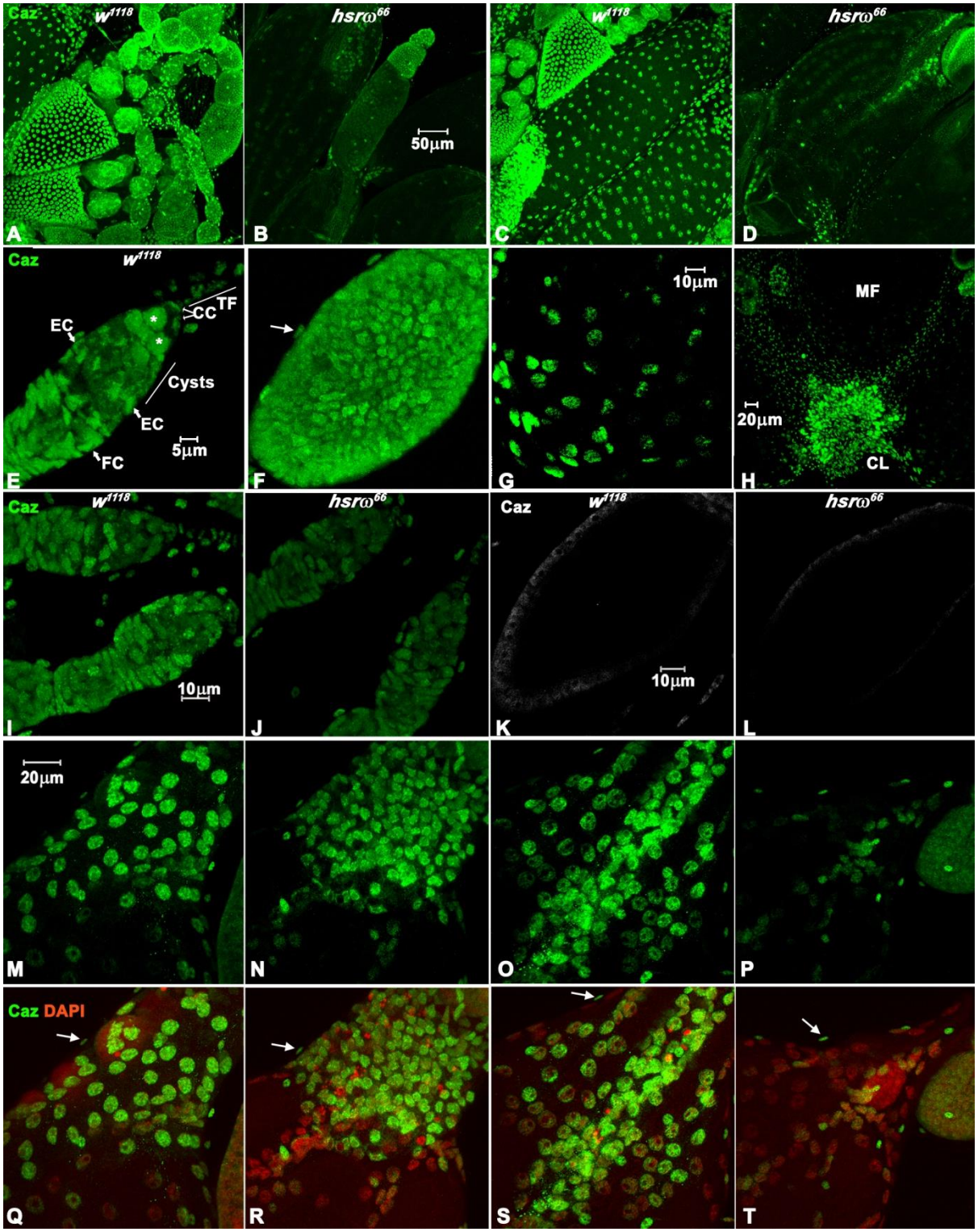

Fig. 7. Caz/dFus hnRNP expression patterns in *w*^{1118} and *hsrω*^{66} ovarioles are generally similar but levels are reduced in *hsrω*^{66} ovaries. (A-D) Confocal projection images of Caz stained (green) ovarioles from 6day old *w*^{1118} (**A,** and **C**) and *hsrω*^{66} (**B,** and **D**) developing (**A-B**) and mature (**C-D**) egg chambers. **(E-H)** Higher magnification confocal projection images of Caz stained (green) germaria (**E**), mid-stage egg chamber (**F**) and posterior follicle cells of mature follicle (**G**), and corpus luteum (**H**) from 6day old *w*^{1118} females; CC = cap cells, EC = escort cells, FC = follicle cells, NC = nurse cells, TF = terminal filament; early cysts and terminal filament are indicated by white lines,

and GSCs are marked by '*', respectively in (**E**); white arrow in **F** indicates an ovarian sheath cell; MF = mature follicle; CL = corpus luteum in **H**. (**I-J**) Confocal projection images of Caz stained (green) germaria from 6day old w^{1118} (**I**) and $hsr\omega^{66}$ (**J**). (**K-L**) Optical sections of Caz (white) stained mid-stage egg chambers showing presence of Caz in follicle but not in nurse cells in w^{1118} (**K**) and $hsr\omega^{66}$ (**L**). (**M-N**) Confocal projection images showing Caz (green) in anterior follicle cells of early stage 14 mature follicles from w^{1118} (**M**) and $hsr\omega^{66}$ ovaries (**N**); (**O-P**) Confocal projection images of Caz stained (green) anterior follicle cells of late stage 14 mature follicles from ovaries of w^{1118} (**O**) and $hsr\omega^{66}$ (**P**) females. (**Q-T**) are DAPI (red) counter-stained images of **M-P**, respectively; white arrows in **Q**, **R**, **S**, and **T** point to Caz-rich ovarian sheath cells. Scale bar in **B** = 50µm and applies to **A-D**, in **E** = 5µm and applies to **E-F**, in **G** = 10µm, in **H** = 20µm, in **I** = 10µm and applies to **I-J**, in **K** = 10µm and applies to **K-L**, and in **M** = 20µm, and applies to **M-T**.

Effects of down-regulation of Caz on oogenesis in *tjGAL4>cazRNAi* females without or with altered levels of *hsrω* transcripts were next examined (Fig. 8). As noted above the Caz expression pattern from germarium to mid-oogenesis was comparable in the $hsr\omega^{66}$ (Fig. 7B, J, and L) and w^{1118} (Fig. 7A, I, and K), with Caz being pre-dominantly expressed in the somatic follicle cells. As expected, Caz staining was absent in follicle cells in *tjGAL4>UAS-cazRNAi* early-, mid- and late-stage egg chambers (Fig. 8E, and Fig. 5E-F). Surprisingly however, following its downregulation in somatic follicle cells, Caz expression was highly upregulated in the germline nurse cells and growing oocyte, with predominant location in cytoplasm (Fig. 8E, and Fig. 5E-F). Despite the changes in Caz distribution in *tjGAL4>UAS-cazRNAi* ovaries, these females laid eggs, which despite a slightly reduced antero-posterior axis length, hatched.

Phenotypes of *tjGAL4>cazRNAi/*$hsr\omega^{66}$ (heterozygous for $hsr\omega^{66}$) and *tjGAL4>cazRNAi/hsrωRNAi* (Fig. 8F, G, J, and K) ovarioles were generally like those seen in *tjGAL4>cazRNAi* ovaries, with Caz present in nurse cells in mid-stage chambers as in *tjGAL4>cazRNAi*. Interestingly, ovaries in *tjGAL4>cazRNAi/EP93D* appeared better since lengths of mature follicles and eggs were nearly like those in wild type (Fig. 8D, H). It may be noted that since the *cazRNAi* transgene is inserted on chromosome 3, effects of *tjGAL4>cazRNAi* on $hsr\omega^{66}$ homozygous condition were not examined.

TBPH/TDP-43

TBPH/TDP-43 is a highly conserved and ubiquitously expressed ribonucleoprotein whose pathological modification is associated with neurodegenerative diseases including amyotrophic lateral sclerosis (ALS) (Kwong et al., 2007; Sreedharan et al., 2008) and whose loss in flies is associated with reduced life span, neuromuscular junction defects and deficient locomotory behaviour, and reduced lifespan in flies (Feiguin et al., 2009). Since TBPH is a component of ω-speckles (Lo Piccolo et al., 2018), its interaction with *hsrω* transcripts during oogenesis was also examined. Down-regulation of TBPH with *tjGAL4* (*tjGAL4>TBPHRNAi*) caused ovulation block without an appreciable effect on early and mid-stage chambers (Fig. 8M, N). Interestingly, co-down regulation of TBPH and *hsrω* transcripts (*tjGAL4>TBPHRNAi; hsrωRNAi*) rescued the ovulation block so that these flies laid normal eggs (Fig. 12O, P).

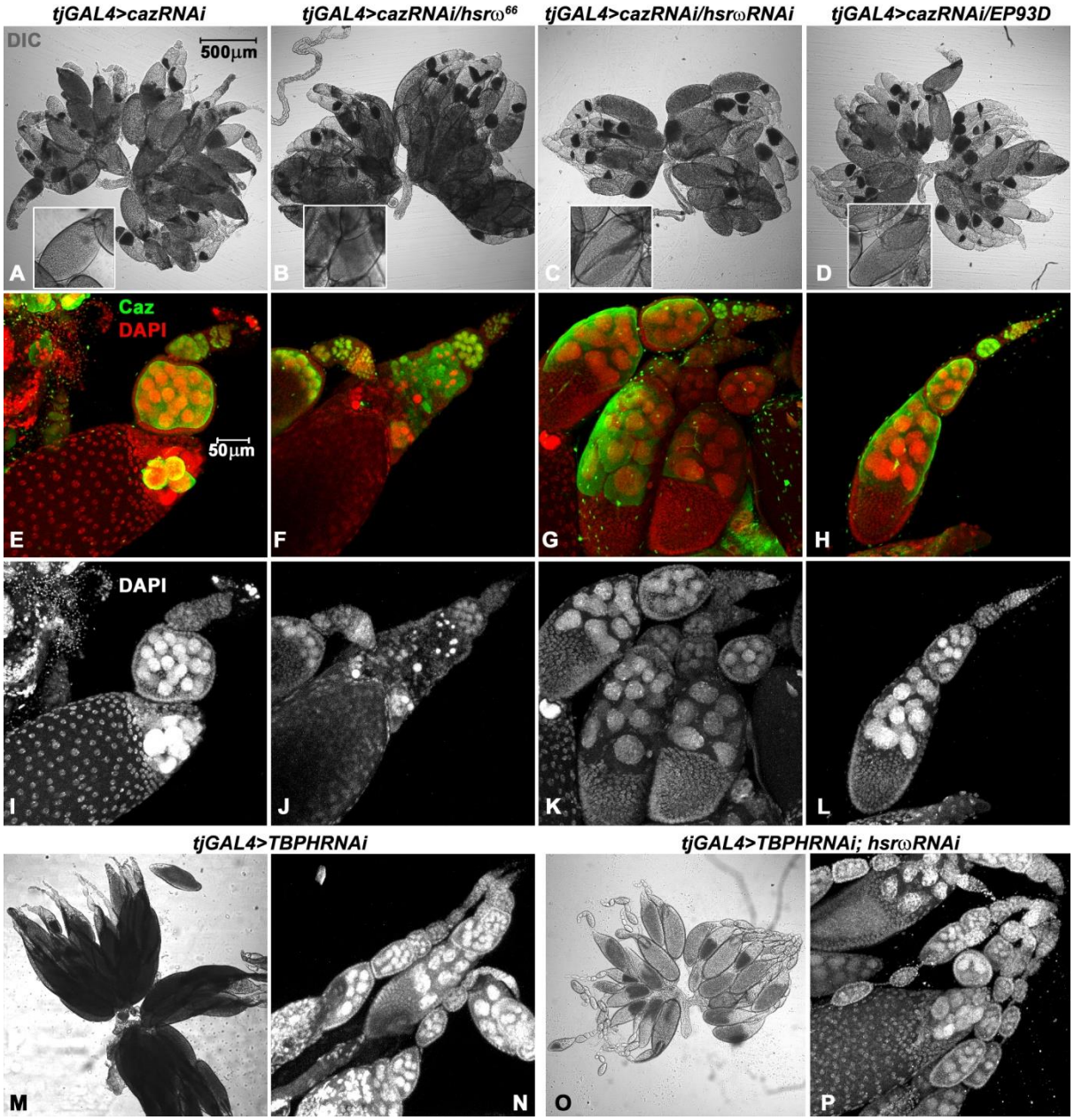

Fig. 8. Targeted knock-down of TBPH (TDP-43), but not Caz, in follicle cells leads to ovulation block which is rescued by *hsrω* down-regulation. (A-D) DIC images of ovaries expressing *tjGAL4>cazRNAi* without or with altered levels of *hsrω* transcripts (genotypes noted above each column); insets show the mature eggs in follicles in each case. **(E-L)** Confocal projection images of Caz (green) and DAPI (red) stained, *tjGAL4>UAS-cazRNAi* ovaries without or with altered levels of *hsrω* transcripts (genotypes as noted above each column); **I-L** show only DAPI (white) staining of chambers in **E-H**, respectively. (**M-N**) DIC (**M**) and DAPI stained (**B**, white, confocal projection) images of *tjGAL4>TBPHRNAi* ovaries. (**O-P**) DIC (**O**) and DAPI stained (**P**, white, confocal projection) images of *tjGAL4>TBPHRNAi/hsrωRNAi* ovaries. Scale bar in **A** = 500μm and applies to **A-D**, and **M**, and **O**; in **I** =50 μm and applies to **E-L**, and **N**, and P.

3.2.7. 20-hyrdoxy-ecdysone (20-HE) feeding partially rescued ovulation block in *hsrω*^{66} females

Ecdysteroids are crucial for *Drosophila* ovulation (Knapp and Sun, 2017). Therefore, to check if the ovarian defects in *hsrω*^{66} females could be due to ecdysone deficiency, the *w*^{1118} and *hsrω*^{66}

male and female flies were fed on 20-HE (0.05mM) supplemented food from 3rd to 8th day after eclosion (total 115 hours of feeding), and their ovaries examined on day 8. The 20-HE feeding had no adverse effect on oogenesis in w^{1118} females (Fig. 9A, C, C', E). Interestingly, however, the 20-HE feeding substantially improved the progression of oogenesis in $hsr\omega^{66}$ females since out of the 50 ovaries examined from 20-HE-fed 25 $hsr\omega^{66}$ females, ovulation block phenotype was not seen in 60% ovaries while 80% of the ovaries also showed presence of apparently normal mid-stage egg chambers (Fig. 9D-D'), which, as noted above, are rare in $hsr\omega^{66}$. The F-actin staining, however, remained weaker in all oogenesis stages in 20-HE fed than in w^{1118} females (Fig. 3D-F). Compared to the $hsr\omega^{66}$ females not fed on 20-HE, those which received the 20-HE supplement, showed better survival, and laid more eggs (data not presented).

Targeted expression of *hsrωRH* transcript in $hsr\omega^{66}$ substantially improved progression of oogenesis

In order to check if the defective oogenesis in $hsr\omega^{66}$ ovaries can be rescued by supplementing some of the *hsrω* transcripts through an inducible transgene the *UAS-hsrωRH* transgene, inserted on chromosome 3 and which expresses the RH transcript of *hsrω* gene under *UAS* promoter (Sahu et al., 2021), was recombined with the $hsr\omega^{66}$ allele to generate *UAS-hsrωRH* $hsr\omega^{66}$ stock. When the *UAS-hsrωRH* transgene was driven by *tjGAL4* or *ActGAL4* in *UAS-hsrωRH* $hsr\omega^{66}$ flies, there was some improvement of survival of early and mid-stage chambers, but the ovulation block persisted (Fig. 9G, H); the rescue was more pronounced in *ActGAL4>UAS-hsrωRH* $hsr\omega^{66}$ than in *tjGAL4>UAS-hsrωRH* $hsr\omega^{66}$ ovaries. Interestingly, a combination of *ActGAL4* and *tjGAL4* drivers in *UAS-hsrωRH* $hsr\omega^{66}$ females (*ActGAL4/tjGAL4>UAS-hsrωRH* $hsr\omega^{66}$) led to a substantial recovery in oogenesis (N=20 ovaries) since the defects typically seen in $hsr\omega^{66}$ females were largely absent. (Fig. 9I). The mean number of ovarioles in *ActGAL4/tjGAL4>UAS-hsrωRH* $hsr\omega^{66}$ ovaries on day6 was 15.35 ($\pm$0.15 S.E.) while the mean % apoptotic egg chambers per ovariole was reduced to 4.89 ($\pm$0.37 S.E.). These values are comparable to the respective values for w^{1118} control females as noted earlier (Fig. 1M, N). The ovulation block seen in $hsr\omega^{66}$ homozygous ovaries was also nearly completely rescued by expression *UAS-UHRH* transgene under combination of *ActGAL4* and *tjGAL4* drivers.

In agreement with the above, immunostaining for Caz or Phalloidin staining for F-actin in ovaries of these three genotypes also confirmed the differential restoration of Caz expression and F-actin levels during oogenesis. Thus, while the Caz or F-actin staining in *tjGAL4>UAS-hsrωRH* $hsr\omega^{66}$ ovarioles remained very low, those in *ActGAL4>UAS-hsrωRH* $hsr\omega^{66}$ and *ActGAL4/tjGAL4>UAS-hsrωRH* $hsr\omega^{66}$ ovaries showed progressively beter improvements (Fig. 9J-R), with the *ActGAL4/tjGAL4>UAS-hsrωRH* $hsr\omega^{66}$ ovarioles showing near normal distribution as noted above in w^{1118} ovaries (Figs. 3.3 and 3.7).

A summary of the various observations reported in this study is presented in Supplementary Table S1.

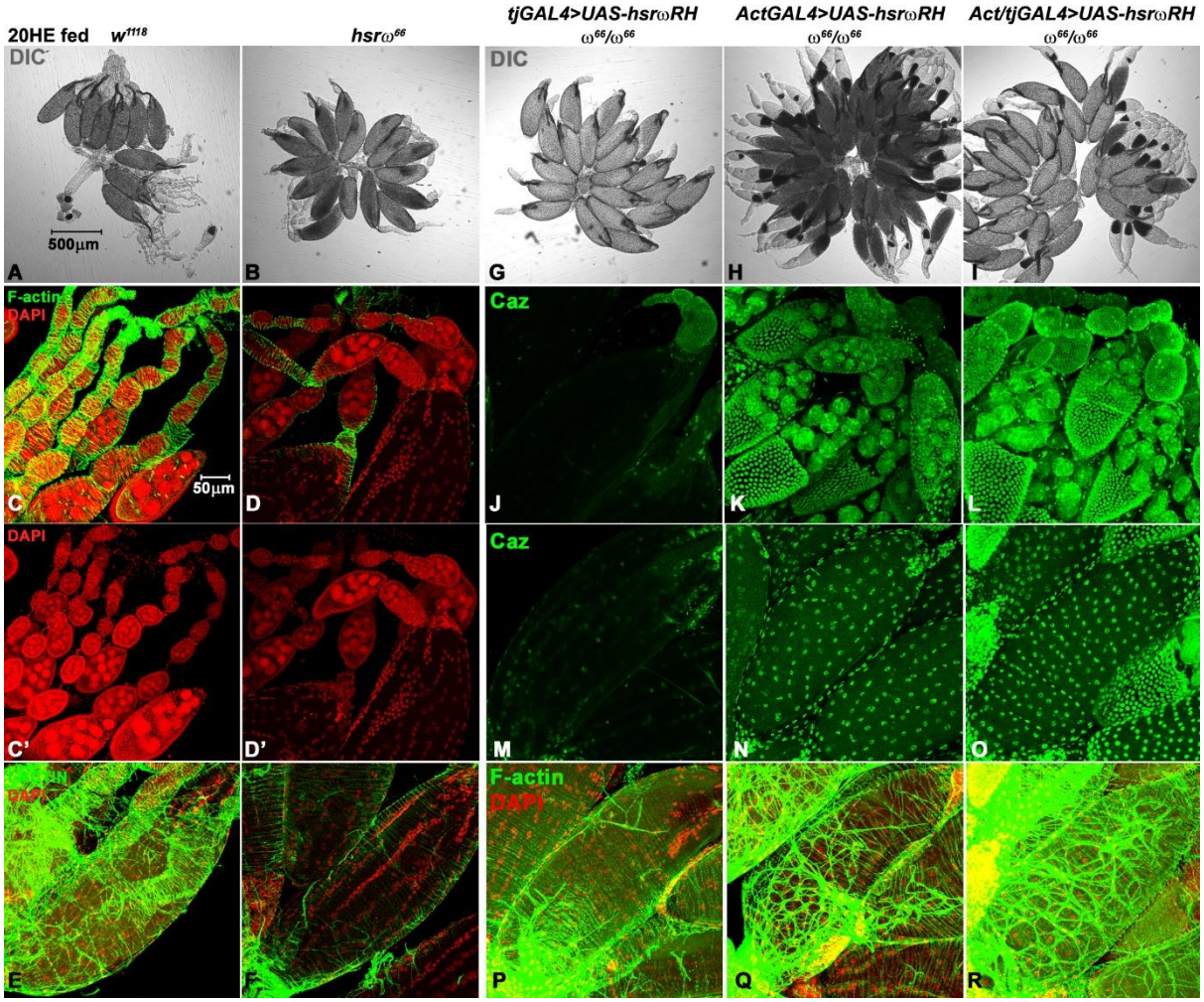

Fig. 9. 20-HE feeding or targeted expression of *hsrω-RH* transcripts partially or substantially rescues oogenesis in *hsrω^{66}* homozygous ovaries. (A-B) DIC images of ovaries from 8 days old *w^{1118}* (**A**) and *hsrω^{66}* (**B**) 20-HE fed females. (**C-F**) Confocal projection images of Phalloidin (green, F-actin) and DAPI (red) stained early- and mid-stage (**C-D'**), and late-stage (**E-F**) egg chambers from 20HE fed *w^{1118}* (**C, C', E**) and *hsrω^{66}* (**D, D', F**) females; **C'** and **D'** show only DAPI stained images of ovarioles in **C** and **D**, respectively. **(G-I)** DIC images of 8 days old *tjGAL4>UAS-hsrωRH hsrω^{66}* (**G**), *ActGAL4>UAS-hsrωRH hsrω^{66}* (**H**), and *ActGAL4/tjGAL4>UAS-hsrωRH hsrω^{66}* (**I**) ovaries showing little (**G**), moderate (**H**) and substantial (**I**) rescue of oogenesis, including alleviation of the ovulation block. **(J-O)** Confocal projection images of Caz (green) stained ovarioles from early to mid (**J-L**) and late stage (**M-O**) chambers in *tjGAL4>UAS-hsrωRH hsrω^{66}* (**J, M**), *ActGAL4>UAS-hsrωRH hsrω^{66}* (**K, N**), and *ActGAL4/tjGAL4>UAS-hsrωRH hsrω^{66}* (**L, O**) ovaries. **(P-R)** Phalloidin (green, F-actin) and DAPI (red) stained images of mature follicles in *tjGAL4>UAS-hsrωRH hsrω^{66}* (**P**), *ActGAL4>UAS-hsrωRH hsrω^{66}* (**Q**), and *ActGAL4/tjGAL4>UAS-hsrωRH hsrω^{66}* (**R**) ovaries. Scale bar in **A** = 500µm and applies to **A, B** and **G-I** while that in **D =** 50µm and applies to **C-F** and **J-R**.

Discussion

Mis-expression of the multiple lncRNA encoding *hsrω* gene of *Drosophila melanogaster* exerts pleiotropic effects on different life-history parameters and cell stress response (Lakhotia et al., 2012; Mallik and Lakhotia, 2011; Singh and Lakhotia, 2015). The present observation

that life span and female fecundity are significantly reduced in *hsrω*^{66} homozygous flies, which have very low amounts of this gene's different transcripts (Ray et al., 2019a), agrees with earlier reports that loss of function of *hsrω* is associated with highly reduced embryonic viability with the few survivors being weak and short-lived (Estes et al., 2011; Johnson et al., 2011; Lo Piccolo and Yamaguchi, 2017; Mohler and Pardue, 1982; Ray and Lakhotia, 1998). The significantly shortened life span of *hsrω* ^{66} flies also agrees with a recent report (Davie et al., 2018) that *hsrω* transcripts are greatly reduced with age and that this locus is one of the most important genes affecting ageing. Further reduction in life span and fecundity of *hsrω*^{66} females when kept with *w*^{1118} males is intriguing. Mating is known to affect physiology in multiple ways, including life span of *Drosophila* females, through pheromones and seminal fluid proteins (Barnes et al., 2008; Koliada et al., 2020; Patlar and Civetta, 2022). This interesting observation needs further examination to see if the male's behaviour or seminal fluid components or both have a role in the premature death of *hsrω*^{66} females following their mating with *w*^{1118} males. Since *hsrω* ^{66} males did not affect fertility of *w*^{1118} females, the near absence of *hsrω* transcripts does not seem to greatly affect spermatogenesis. In agreement, unlike the grossly affected ovaries in *hsrω* ^{66} females, testes in *hsrω* ^{66} males appeared normal (not shown).

The *hsrω* transcripts are present in nearly all stages of oogenesis (Mutsuddi and Lakhotia, 1995). One of the major pathways through which the *hsrω* nuclear lncRNAs act is through modulation of intra-cellular dynamics of several RNA binding proteins, the most prominent being the diverse hnRNPs (Lakhotia, 2011; Lakhotia et al., 2012; Lo Piccolo et al., 2014; Prasanth et al., 2000; Singh and Lakhotia, 2015), which have major roles in regulation of gene expression, processing of pre-mRNAs and transport of mRNAs (Chaudhury et al., 2010; Lin et al., 2015; Lo Piccolo et al., 2014). Since different hnRNPs have significant roles in specific stages of *Drosophila* oogenesis (Bansal et al., 2020; Casale et al., 2019; Dutta et al., 2020; Finger et al., 2022; Lasko, 2003; Peng and Gavis, 2022; Singh and Lakhotia, 2012), perturbations in hnRNP dynamics due to disruptions of *hsrω* gene activity are likely to have wide-ranging pleiotropic consequences (Mallik and Lakhotia, 2011). The recently identified hnRNP interactors of *hsrω*, the TBPH/TDP-43 and Caz/dFus have wide-ranging roles in transcriptional and translational regulations and mis-expression of either of them is implicated as the major causal factor for neuro-muscular disorders like Frontotemporal lobar degeneration and Amylotropic lateral sclerosis (Chung et al., 2018; Lo Piccolo et al., 2014; Lo Piccolo et al., 2017; Lo Piccolo et al., 2019; Lo Piccolo and Yamaguchi, 2017). Down-regulation of *hsrω* transcripts affects their sub-cellular localization, which is also associated with weaker neuromuscular junctions (Chung et al., 2018; Lo Piccolo and Yamaguchi, 2017). The altered metabolism of proteins like TBPH/TDP-43 and Caz/dFus in *hsrω* ^{66} flies with greatly reduced *hsrω* transcripts may thus be a major contributor to their weak neuro-muscular activities and lifespan. Besides their poor viability, shorter life span and mobility defects, the *hsrω*^{66} individuals appeared to have poor feeding-ability (data not shown). The consequent poor nutritional status may also adversely affect oogenesis through organismic level de-regulation of hormonal and paracrine signaling (Drummond-Barbosa and Spradling, 2001; Liao and Nässel, 2020; Meiselman et al., 2018).

It is interesting that unlike the grossly defective oogenesis in *hsrω*^{66} females, ovarian development was only partially affected when the *UAS-hsrωRNAi* transgene was expressed under the ubiquitous *daGAL4* driver (Chaturvedi et al., 2016). This difference between *hsrω*^{66} and *daGAL4>UAS-hsrωRNAi* ovaries presumably relates to the fact that unlike all transcripts of this gene being nearly absent in the *hsrω*^{66} homozygotes, *UAS-hsrωRNAi* transgene expression primarily targets this gene's long nuclear transcripts (Mallik and Lakhotia, 2009) and despite the down-regulation, levels of the target transcripts remain much higher than in

hsrω^{66} (Ray et al., 2019a). Additionally, the *UAS-hsrωRNAi* transgene's expression in ovaries under the *daGAL4* driver may be mostly limited to somatic follicle cells since the *UAS-hsrωRNAi* transgene is cloned in *pUAST* vector (Mallik and Lakhotia, 2009), which may not efficiently respond to the GAL4 in germline cells (DeLuca and Spradling, 2018). Despite these limitations, expression of the *UAS-hsrωRNAi* transgene under *daGAL4* driver resulted in substantial apoptosis of mid-stage egg chambers, confirming that this lncRNA gene has important roles in oogenesis.

The delayed and poor egg-laying capacity of *hsrω*^{66} young females relates with their small ovaries and reduced numbers of ovarioles in freshly emerged flies and the slow progress of follicle development. The oviposition patterns of the mutant flies and development of ovarian follicles in *hsrω*^{66} flies on different days after eclosion indicate that a paucity of *hsrω* transcripts delays the initial phase of follicle development, which starts only from day 3 onwards. This initial wave of egg chamber development results in productive ovulation letting these females successfully lay eggs between days 6-8, although the number is only ~1/3rd of those laid by *w*^{1118} flies. However, soon after this initial phase, ovulation block occurs, which seems to suppress development of the existing early-stage follicles through feedback regulation (Drummond-Barbosa and Spradling, 2001; Meiselman et al., 2018) so that beyond day 6 very few stage 7-13 chambers are seen in *hsrω*^{66} ovaries.

Although the TF, CC and GSC numbers were not significantly affected in *hsrω*^{66} germaria of 6day old females, levels of Vasa and fusomes were reduced in cysts and early-stage cysts in day6 *hsrω*^{66} ovarioles. Since fusomes regulate the pattern and synchrony of divisions during egg chamber differentiation, movement of mitochondria through ring canals to the oocyte and roles in various signaling events during follicle growth (Cox and Spradling, 2003; de Cuevas et al., 1996; Lighthouse et al., 2008; Lilly et al., 2000), their perturbed organization in *hsrω*^{66} early-stage cysts would have multiple long-range consequences.

The observed high incidence of apoptosis in mid-stage egg chambers, a quality-control check-point (Lebo and McCall, 2021), in *hsrω*^{66} and *daGAL4>hsrωRNAi* ovaries clearly shows that egg chamber development is severely compromised in the absence of these transcripts. The high apoptosis at mid-oogenesis step also contributes to the paucity of stage 10-13 chambers in these mutants. Despite fewer stage 10-13 chambers following very high frequency of apoptosis of mid-stage chambers in *daGAL4>hsrωRNAi* expressing ovaries, they continue to produce and lay some mature eggs since the ovariole number is not reduced and ovulation block is mild..

We examined involvement of Notch and Cut signaling in ovaries with altered *hsrω* transcripts since these are major regulators of oogenesis and ovulation (Deady et al., 2017; Jackson and Blochlinger, 1997; Sun and Deng, 2005). Our results with over-expression of active Notch in follicle cells using the *tj-GAL4* driver suggest that since neither down- nor up-regulation of *hsrω* transcripts affected the *tjGAL4>UAS-Notch*^{Act} ovarian phenotype, the *hsrω* transcripts in *hsrω*^{66} or *tjGAL4>hsrωRNAi* or *tjGAL4>EP93D* ovaries may not act upstream of the Notch signaling in follicle cells. On the other hand, present results showed that the expression of Cut, a homeodomain protein regulating soma-to-germline signaling pathway and chorion gene amplification in follicle cells (Jackson and Berg, 1999; Jackson and Blochlinger, 1997), is reduced in *hsrω*^{66} ovaries, which suggests some involvement of these transcripts in Cut expression. The modulation of effects of the *tjGAL4* driven down- or up-regulation of Cut in ovarian follicle cells by the altered levels of *hsrω* transcripts suggests that Cut may also affect activities of these transcripts. An interaction of Cut and *hsrω* is indicated by some similarities in defects seen in *hsrω*^{66} mid-stage egg chambers and those following disruption of Cut expression. The finding that low levels of *hsrω* transcripts in *hsrω*^{66} or following expression

of *hsrωRNAi* transgene did not modify the ovarian phenotypes due to *tjGAL4* driven down- or up-regulation of Cut suggest that low as well as high levels of Cut in follicle cells may reduce levels of *hsrω* transcripts so that any further reduction of these transcripts may remain ineffective. This is supported by our finding that over-expression of *hsrω* transcripts through the GAL4-responsive *EP93D* allele (Mallik and Lakhotia, 2009; Sengupta and Lakhotia, 2006) at least partially rescued the ovarian phenotypes caused by down- or up-regulation of Cut.

The Cut transcription factor also affects ovulation in *Drosophila*, the most strongly affected event in ovarioles with down- or up-regulated levels of *hsrω* transcripts. A down-regulation of Cut at stage 14 is essential for expression of Hindsight (Knapp et al., 2019), which in turn activates the membrane bound matrix metalloproteinase 2 for trimming of posterior follicle cells required for ovulation (Deady et al., 2015). In view of this, the comparable Hnt levels in the mature $hsr\omega^{66}$ and w^{1118} follicles were unexpected since the former do not show the expected trimming of posterior follicle cells. Apparently, some other components required for the trimming are affected in the mature $hsr\omega^{66}$ follicles. In light of known roles of Cut in follicle cell development (Jackson and Berg, 1999; Jackson and Blochlinger, 1997), the reduced levels of Cut in follicle cells during stage 11-13 in $hsr\omega^{66}$ may contribute to the irregular arrangements of body and anterior follicle cells, the higher chromatin content in body follicle cells, and the abnormally developed dorsal appendages in mature $hsr\omega^{66}$ follicles. These defects in follicle cells and their organization may also contribute to the ovulation block in $hsr\omega^{66}$ ovaries.

Transcriptomic analysis (Brown et al., 2014) has noted presence of *caz* transcripts in *Drosophila* ovaries. The present study reports for the first time that Caz is indeed widely expressed in germinal as well as somatic cells of the germarium, and early-stage cysts, but only in somatic follicle cells in mid- and late-stage wild type chambers. The significance of its absence in the germline cells beyond the early stages remains to be understood. The generally reduced Caz expression in $hsr\omega^{66}$ 6day ovaries may be related to an earlier (Lo Piccolo et al., 2019) finding that down-regulation of *hsrω* transcripts enhances arginine dimethylation of Caz/dFus and its consequent degradation. In view of the wide expression of Caz in ovarian follicle cells, our finding that *tjGAL4* driven down regulation of its expression in follicle cells did not affect the progression of oogenesis, except for a reduction in antero-posterior (A-P) axis length of the egg follicle, is unexpected. Equally unexpected is that ectopic expression of Caz in nurse cells following its absence in follicle cells of *tjGAL4>cazRNAi* ovarioles did not affect oogenesis. It needs further studies to know if Caz has only some dispensable functions in oogenesis or some other proteins take over its functions in follicle cells when this is not expressed. Absence of ovulation defect in *tjGAL4>cazRNAi* ovarioles indicates that the Caz protein may not be involved in ovulation despite its pronounced presence in the anterior and posterior follicle cells at stage 14. The altered distribution of Caz in *tjGAL4>cazRNAi* ovarioles may be responsible for the reduction of the A-P axis of follicles and egg. Restoration of A-P axis length following over-expression of *hsrω* transcripts in *cazRNAi* expressing follicle cells (*tjGAL4>cazRNAi EP93D*) may be due to a reduced turnover of Caz in the presence of abundant *hsrω* transcripts (Lo Piccolo et al., 2019). While the absence of ovulation block in *tjGAL4>cazRNAi* $hsr\omega^{66}/+$ ovaries is likely due to the presence of one copy of $hsr\omega^{+}$ allele, it is surprising that co-down-regulation of *hsrω* and *caz* transcripts in *tjGAL4>cazRNAi hsrωRNAi* ovaries alleviated the ovulation block seen in *tjGAL4>hsrωRNAi* ovarioles. Presence of ovulation block in *tjGAL4>EP93D* but its absence in *tjGAL4>cazRNAi EP93D* ovaries further reflects a complex interaction between the *hsrω* transcripts and its multiple interacting proteins so that down or up-regulation of these transcripts may not always show the expected opposing effects, and in some cases, the two contrasting conditions may actually result in similar final outcome although through different paths (Lakhotia, 2011; Ray and Lakhotia, 2019; Ray et al., 2019b). The alleviation of ovulation block seen in *tjGAL4>TBPH*

RNAi by co-down-regulation of TBPH and *hsrω* transcripts also reflects complexity of the interactions between *hsrω* transcripts and regulatory factors.

Progression of *Drosophila* oogenesis and the process of ovulation, are highly dependent upon nutritional status of females, conditions of stress, and diverse paracrine and endocrine signaling (Drummond-Barbosa and Spradling, 2001; Kurogi et al., 2021; Liao and Nässel, 2020; Meiselman et al., 2018; Okamoto and Watanabe, 2022; Song and Zhou, 2020; Weaver and Drummond-Barbosa, 2021). The weak and unhealthy condition, short life span etc of the surviving $hsr\omega^{66}$ homozygotes reflect their poor state of general physiology. The *hsrω* gene is abundantly expressed in prothoracic gland (Mutsuddi and Lakhotia, 1995) and affects ecdysone as well Dilp8 signaling (Ray and Lakhotia, 2019; Ray et al., 2019b), both of which affect oogenesis and ovulation in *Drosophila* (Finger et al., 2021; Kurogi et al., 2021; Liao and Nässel, 2020; Meiselman et al., 2018; Weaver and Drummond-Barbosa, 2021). Thus, it is likely that the observed effects on oogenesis in $hsr\omega^{66}$ ovaries may also be due to dysregulated intra- as well as inter-organ communications. The present finding that feeding of $hsr\omega^{66}$ flies on ecdysone supplemented food partially improved their ovarian organization and oogenesis confirms that a near absence of *hsrω* transcripts in $hsr\omega^{66}$ flies reduces ecdysone production and/or the circulating levels. Further studies are required to know if the ecdysone production in brain or ovaries or in both is affected in *hsrω* mis-expressing individuals.

The *hsrω* gene produces at least seven transcripts (www.flybase.org) using two transcription start and four termination sites and variable splicing of its single intron (Sahu et al., 2020). The $hsr\omega^{66}$ homozygotes show extremely low levels of all these transcripts (Ray et al., 2019a). With a view to understand if all or some of these multiple transcripts have roles in *Drosophila* oogenesis, as a first step here we examined effects of expression of the *UAS-hsrωRH* transcripts in $hsr\omega^{66}$ ovarian follicle cells. The RH transcript corresponds to the region between the second transcription start site (TSS2) and second termination site located just before beginning of the 280bp tandem repeats (Sahu et al., 2020). Since the *tjGAL4>hsrωRNAi* or *daGAL4>hsrωRNAi*, which would have primarily affected the long nuclear transcripts containing the 280bp tandem repeats (Mallik and Lakhotia, 2009), did not show as major blocks in oogenesis as in $hsr\omega^{66}$ ovaries, we selected *hsrωRH* transcripts for ectopic expression. Remarkably, while expression of this transgene with either *ActGAL4* or *tjGAL4* driver in $hsr\omega^{66}$ background resulted in only partial improvement in oogenesis, its strnger and wider expression with a combination of *ActGAL4* and *tjGAL4* drivers in $hsr\omega^{66}$ females substantially restored oogenesis, as revealed by the general morphology of *ActGAL4/tjGAL4>UAS-hsrωRH* $hsr\omega^{66}$ ovaries and by the Caz and F-actin expression in them being largely like that in w^{1118} ovaries. It is likely that ectopic expression of the *UAS-hsrωRH* transgene when driven by any one of these two GAL4 drivers remained sub-critical so that all the defects in oogenesis associated with $hsr\omega^{66}$ mutant condition could not be suppressed. Nevertheless, these results reaffirm a causal role of absence of the *hsrω* transcripts in the observed general disruption of oogenesis in $hsr\omega^{66}$ females. Since the *hsrωRH* transcript includes the region present in the *hsrωRC* transcript and that encoding small Omega peptide, the specific contributions of the two transcripts and Omega peptide in restoring oogenesis defects in $hsr\omega^{66}$ ovaries remain unclear. This approach of utilizing the available GAL4-inducible transgenes for specific expression of the other transcripts of this gene (Sahu et al., 2021) provides directions for future studies to explore roles of specific *hsrω* transcripts and the small Omega peptide in oogenesis in *Drosophila*.

The *hsrω* lncRNA gene of *Drosophila melanogaster* is known to have multi-faceted roles in normal development and in cell stress conditions (Lakhotia, 2011; Ray et al., 2019a; Ray et al., 2019b; Singh and Lakhotia, 2015). The present study extends this gene's involvement in oogenesis via intra- as well as inter-organ regulatory events. As expected of a gene producing

multiple transcripts which interact with a wide variety of regulatory and other molecules in cell, the present gene interaction studies did not reveal simple linear causal inter-relations with other potential regulators of oogenesis in *Drosophila.* These results nevertheless open novel possibilities for understanding roles of *hsrω* and other lncRNAs in the complex process of oogenesis

Acknowledgements: RS thanks the Lady Tata Memorial Trust (Mumbai, India) for research fellowship. SCL acknowledges the Science & Engineering Research Board (Govt. of India) for the Distinguished Fellowship. This work was supported by a grant (BT/PR32126/BRB/10/1775/2019) from the Department of Biotechnology, Govt. of India (New Delhi) to SCL. We thank Pralay Majumder (Kolkata, India) and the Bloomington Drosophila Stock Centre (USA) for providing fly stocks as listed in Materials and Methods.

Conflict of Interest: None.

References

Arya, R., Sarkissian, T., Tan, Y., White, K., 2015. Neural stem cell progeny regulate stem cell death in a Notch and Hox dependent manner. Cell Death Differ 22, 1378-1387.

Bansal, P., Madlung, J., Schaaf, K., Macek, B., Bono, F., 2020. An interaction network of RNA-Binding proteins involved in Drosophila Oogenesis. Molecular & Cellular Proteomics 19, 1485-1502.

Barnes, A.I., Wigby, S., Boone, J.M., Partridge, L., Chapman, T., 2008. Feeding, fecundity and lifespan in female *Drosophila melanogaster*. Proceedings of the Royal Society B: Biological Sciences 275, 1675-1683.

Brown, J.B., Boley, N., Eisman, R., May, G.E., Stoiber, M.H., Duff, M.O., Booth, B.W., Wen, J., Park, S., Suzuki, A.M., 2014. Diversity and dynamics of the Drosophila transcriptome. Nature 512, 393-399.

Casale, A.M., Cappucci, U., Fanti, L., Piacentini, L., 2019. Heterochromatin protein 1 (HP1) is intrinsically required for post-transcriptional regulation of Drosophila Germline Stem Cell (GSC) maintenance. Sci Rep 9, 4372.

Chaturvedi, D., Inaba, M., Scoggin, S., Buszczak, M., 2016. Drosophila CG2469 Encodes a Homolog of Human CTR9 and Is Essential for Development. G3 (Bethesda) 6, 3849-3857.

Chaudhury, A., Chander, P., Howe, P.H., 2010. Heterogeneous nuclear ribonucleoproteins (hnRNPs) in cellular processes: Focus on hnRNP E1's multifunctional regulatory roles. Rna 16, 1449-1462.

Chung, C.-Y., Berson, A., Kennerdell, J.R., Sartoris, A., Unger, T., Porta, S., Kim, H.-J., Smith, E.R., Shilatifard, A., Van Deerlin, V., Lee, V.M.Y., Chen-Plotkin, A., Bonini, N.M., 2018. Aberrant activation of non-coding RNA targets of transcriptional elongation complexes contributes to TDP-43 toxicity. Nature Communications 9, 4406.

Cox, R.T., Spradling, A.C., 2003. A Balbiani body and the fusome mediate mitochondrial inheritance during Drosophila oogenesis. Development 130, 1579-1590.

Davie, K., Janssens, J., Koldere, D., De Waegeneer, M., Pech, U., Kreft, Ł., Aibar, S., Makhzami, S., Christiaens, V., Bravo González-Blas, C., Poovathingal, S., Hulselmans, G., Spanier, K.I., Moerman, T., Vanspauwen, B., Geurs, S., Voet, T., Lammertyn, J., Thienpont, B., Liu, S., Konstantinides, N., Fiers, M., Verstreken, P., Aerts, S., 2018. A Single-Cell transcriptome atlas of the aging *Drosophila* brain. Cell 174, 982-998.e920.

de Cuevas, M., Lee, J.K., Spradling, A.C., 1996. alpha-spectrin is required for germline cell division and differentiation in the Drosophila ovary. Development 122, 3959-3968.

Deady, L.D., Li, W., Sun, J., 2017. The zinc-finger transcription factor Hindsight regulates ovulation competency of Drosophila follicles. Elife 6.

Deady, L.D., Shen, W., Mosure, S.A., Spradling, A.C., Sun, J., 2015. Matrix metalloproteinase 2 is required for ovulation and corpus luteum formation in Drosophila. PLoS Genet 11, e1004989.
DeLuca, S.Z., Spradling, A.C., 2018. Efficient Expression of Genes in the Drosophila Germline Using a UAS Promoter Free of Interference by Hsp70 piRNAs. Genetics 209, 381-387.
Drummond-Barbosa, D., Spradling, A.C., 2001. Stem cells and their progeny respond to nutritional changes during Drosophila oogenesis. Dev Biol 231, 265-278.
Dutta, D., Mutsuddi, M., Mukherjee, A., 2020. Regulation of notch signaling in Drosophila melanogaster: The role of the heterogeneous nuclear ribonucleoprotein Hrp48 and Deltex, in: Reichrath, J., Reichrath, S. (Eds.), Notch Signaling in Embryology and Cancer: Molecular Biology of Notch Signaling. Springer International Publishing, Cham, pp. 95-105.
Eliazer, S., Buszczak, M., 2011. Finding a niche: studies from the Drosophila ovary. Stem Cell Res Ther 2, 45.
Estes, P.S., Boehringer, A., Zwick, R., Tang, J.E., Grigsby, B., Zarnescu, D.C., 2011. Wild-type and A315T mutant TDP-43 exert differential neurotoxicity in a Drosophila model of ALS. Human Molecular Genetics 20, 2308-2321.
Feiguin, F., Godena, V.K., Romano, G., D'Ambrogio, A., Klima, R., Baralle, F.E., 2009. Depletion of TDP-43 affects Drosophila motoneurons terminal synapsis and locomotive behavior. FEBS Lett 583, 1586-1592.
Finger, D.S., Whitehead, K.M., Phipps, D.N., Ables, E.T., 2021. Nuclear receptors linking physiology and germline stem cells in Drosophila, in: Litwack, G. (Ed.), Vitamins and Hormones. Academic Press, pp. 327-362.
Finger, D.S., Williams, A.E., Holt, V.V., Ables, E.T., 2022. Novel roles for RNA binding proteins squid, hephaesteus, and Hrb27C in Drosophila oogenesis. Dev Dyn.
Greenbaum, M.P., Iwamori, T., Buchold, G.M., Matzuk, M.M., 2011. Germ cell intercellular bridges. Cold Spring Harb Perspect Biol 3, a005850.
Hongay, C.F., Orr-Weaver, T.L., 2011. Drosophila Inducer of MEiosis 4 (IME4) is required for Notch signaling during oogenesis. Proc Natl Acad Sci U S A 108, 14855-14860.
Jackson, S.M., Berg, C.A., 1999. Soma-to-germline interactions during Drosophila oogenesis are influenced by dose-sensitive interactions between cut and the genes cappuccino, ovarian tumor and agnostic. Genetics 153, 289-303.
Jackson, S.M., Blochlinger, K., 1997. cut interacts with Notch and protein kinase A to regulate egg chamber formation and to maintain germline cyst integrity during Drosophila oogenesis. Development 124, 3663-3672.
Johnson, T.K., Cockerell, F.E., McKechnie, S.W., 2011. Transcripts from the Drosophila heat-shock gene hsr-omega influence rates of protein synthesis but hardly affect resistance to heat knockdown. Mol Genet Genomics 285, 313-323.
Kirilly, D., Xie, T., 2007. The Drosophila ovary: an active stem cell community. Cell Res 17, 15-25.
Knapp, E., Sun, J., 2017. Steroid signaling in mature follicles is important for Drosophila ovulation. Proc Natl Acad Sci U S A 114, 699-704.
Knapp, E.M., Li, W., Sun, J., 2019. Downregulation of homeodomain protein Cut is essential for Drosophila follicle maturation and ovulation. Development 146.
Koliada, A., Gavrilyuk, K., Burdylyuk, N., Strilbytska, O., Storey, K.B., Kuharskii, V., Lushchak, O., Vaiserman, A., 2020. Mating status affects Drosophila lifespan, metabolism and antioxidant system. Comparative Biochemistry and Physiology Part A: Molecular & Integrative Physiology 246, 110716.
Kurogi, Y., Mizuno, Y., Imura, E., Niwa, R., 2021. Neuroendocrine regulation of reproductive dormancy in the fruit fly Drosophila melanogaster: A review of juvenile hormone-dependent regulation. Frontiers in Ecology and Evolution 9, 715029.

Kwong, L.K., Neumann, M., Sampathu, D.M., Lee, V.M., Trojanowski, J.Q., 2007. TDP-43 proteinopathy: the neuropathology underlying major forms of sporadic and familial frontotemporal lobar degeneration and motor neuron disease. Acta Neuropathol 114, 63-70.
Lakhotia, S.C., 2011. Forty years of the 93D puff of Drosophila melanogaster. J. Biosciences 36, 399-423.
Lakhotia, S.C., Mallik, M., Singh, A.K., Ray, M., 2012. The large noncoding hsrω-n transcripts are essential for thermotolerance and remobilization of hnRNPs, HP1 and RNA polymerase II during recovery from heat shock in Drosophila. Chromosoma 121, 49-70.
Lanson, N.A., Jr., Maltare, A., King, H., Smith, R., Kim, J.H., Taylor, J.P., Lloyd, T.E., Pandey, U.B., 2011. A Drosophila model of FUS-related neurodegeneration reveals genetic interaction between FUS and TDP-43. Hum Mol Genet 20, 2510-2523.
Lasko, P., 2003. Cup-ling oskar RNA localization and translational control. J Cell Biol 163, 1189-1191.
Lebo, D.P.V., McCall, K., 2021. Murder on the ovarian express: A tale of non-autonomous cell death in the Drosophila ovary. Cells 10, 1454.
Lee, J.K., Brandin, E., Branton, D., Goldstein, L.S., 1997. alpha-Spectrin is required for ovarian follicle monolayer integrity in Drosophila melanogaster. Development 124, 353-362.
Liao, S., Nässel, D.R., 2020. Drosophila insulin-like peptide 8 (DILP8) in ovarian follicle cells regulates ovulation and metabolism. Frontiers in Endocrinology 11, 461.
Lighthouse, D.V., Buszczak, M., Spradling, A.C., 2008. New components of the Drosophila fusome suggest it plays novel roles in signaling and transport. Dev Biol 317, 59-71.
Lilly, M.A., de Cuevas, M., Spradling, A.C., 2000. Cyclin A associates with the fusome during germline cyst formation in the Drosophila ovary. Dev Biol 218, 53-63.
Lin, Y., Protter, D.S., Rosen, M.K., Parker, R., 2015. Formation and Maturation of Phase-Separated Liquid Droplets by RNA-Binding Proteins. Mol Cell 60, 208-219.
Lo Piccolo, L., Bonaccorso, R., Attardi, A., Li Greci, L., Romano, G., Sollazzo, M., Giurato, G., Ingrassia, A.M.R., Feiguin, F., Corona, D.F.V., Onorati, M.C., 2018. Loss of ISWI Function in Drosophila Nuclear Bodies Drives Cytoplasmic Redistribution of Drosophila TDP-43. Int J Mol Sci 19.
Lo Piccolo, L., Corona, D., Onorati, M.C., 2014. Emerging roles for hnRNPs in post-transcriptional regulation: what can we learn from flies? Chromosoma 123, 515-527.
Lo Piccolo, L., Jantrapirom, S., Nagai, Y., Yamaguchi, M., 2017. FUS toxicity is rescued by the modulation of lncRNA hsrω expression in Drosophila melanogaster. Scientific reports 7, 15660.
Lo Piccolo, L., Mochizuki, H., Nagai, Y., 2019. The lncRNA hsrω regulates arginine dimethylation of human FUS to cause its proteasomal degradation in Drosophila. Journal of Cell Science 132, jcs236836.
Lo Piccolo, L., Yamaguchi, M., 2017. RNAi of arcRNA hsrω affects sub-cellular localization of Drosophila FUS to drive neurodiseases. Exp Neurol 292, 125-134.
Mallik, M., Catinozzi, M., Hug, C.B., Zhang, L., Wagner, M., Bussmann, J., Bittern, J., Mersmann, S., Klämbt, C., Drexler, H.C.A., Huynen, M.A., Vaquerizas, J.M., Storkebaum, E., 2018. Xrp1 genetically interacts with the ALS-associated FUS orthologue caz and mediates its toxicity. J Cell Biol 217, 3947-3964.
Mallik, M., Lakhotia, S.C., 2009. RNAi for the large non-coding hsr omega transcripts suppresses polyglutamine pathogenesis in *Drosophila* models. RNA Biol 6, 464-478.
Mallik, M., Lakhotia, S.C., 2011. Pleiotropic consequences of misexpression of the developmentally active and stress-inducible non-coding hsrω gene in Drosophila. J Biosci 36, 265-280.

Meiselman, M.R., Kingan, T.G., Adams, M.E., 2018. Stress-induced reproductive arrest in Drosophila occurs through ETH deficiency-mediated suppression of oogenesis and ovulation. BMC Biol 16, 18.
Mohler, J., Pardue, M.L., 1982. Deficiency mapping of the 93D heat-shock locus in *Drosophila melanogaster*. Chromosoma 86, 457-467.
Mutsuddi, M., Lakhotia, S.C., 1995. Spatial expression of the hsr-omega (93D) gene in different tissues of Drosophila melanogaster and identification of promoter elements controlling its developmental expression. Dev Genet 17, 303-311.
Nystul, T., Spradling, A., 2010. Regulation of epithelial stem cell replacement and follicle formation in the Drosophila ovary. Genetics 184, 503-515.
Okamoto, N., Watanabe, A., 2022. Interorgan communication through peripherally derived peptide hormones in Drosophila. Fly 16, 152-176.
Patlar, B., Civetta, A., 2022. Seminal fluid gene expression and reproductive fitness in Drosophila melanogaster. BMC Ecology and Evolution 22, 20.
Peng, Y., Gavis, E.R., 2022. The Drosophila hnRNP F/H homolog Glorund recruits dFMRP to inhibit nanos translation elongation. Nucleic Acids Research 50, 7067-7083.
Prasanth, K.V., Rajendra, T.K., Lal, A.K., Lakhotia, S.C., 2000. Omega speckles - a novel class of nuclear speckles containing hnRNPs associated with noncoding hsr-omega RNA in Drosophila. J Cell Sci 113 Pt 19, 3485-3497.
Pritchett, T., McCall, K., 2012. Role of the insulin/Tor signaling network in starvation-induced programmed cell death in Drosophila oogenesis. Cell Death & Differentiation 19, 1069-1079.
Ray, M., Acharya, S., Shambhavi, S., Lakhotia, S.C., 2019a. Over-expression of Hsp83 in grossly depleted hsrω lncRNA background causes synthetic lethality and l(2)gl phenocopy in Drosophila. J Biosci 44, 36, DOI:10.1007/s12038-12019-19852-z.
Ray, M., Lakhotia, S.C., 2019. Activated Ras/JNK driven Dilp8 in imaginal discs adversely affects organismal homeostasis during early pupal stage in Drosophila, a new checkpoint for development. Developmental Dynamics 248, 1211-1231.
Ray, M., Singh, G., Lakhotia, S.C., 2019b. Altered levels of hsromega lncRNAs further enhance Ras signaling during ectopically activated Ras induced R7 differentiation in Drosophila. Gene Expression Patterns 33, 20-36.
Ray, P., Lakhotia, S.C., 1998. Interaction of the non-protein-coding and stress-inducible hsrw gene with *Ras* genes of *Drosophila melanogaster*. J Biosci 4, 377-386.
Sahu, R.K., Mutt, E., Lakhotia, S.C., 2020. Conservation of gene architecture and domains amidst sequence divergence in the hsrω lncRNA gene across the Drosophila genus: an in silico analysis. Journal of Genetics 99, 64.
Sahu, R.K., Trivedi, D., Lakhotia, S.C., 2021. Transgenic resources for functional studies on the hsrω gene in Drosophila. DIS 121, 34-41.
Sengupta, S., Lakhotia, S.C., 2006. Altered expressions of the noncoding hsromega gene enhances poly-Q-induced neurotoxicity in Drosophila. RNA Biol 3, 28-35.
Singh, A.K., Lakhotia, S.C., 2012. The hnRNP A1 homolog Hrp36 is essential for normal development, female fecundity, omega speckle formation and stress tolerance in Drosophila melanogaster. J Biosci 37, 659-678.
Singh, A.K., Lakhotia, S.C., 2015. Dynamics of hnRNPs and omega speckles in normal and heat shocked live cell nuclei of Drosophila melanogaster. Chromosoma 124, 367-383.
Snapp, E.L., Iida, T., Frescas, D., Lippincott-Schwartz, J., Lilly, M.A., 2004. The fusome mediates intercellular endoplasmic reticulum connectivity in Drosophila ovarian cysts. Mol Biol Cell 15, 4512-4521.
Song, J., Zhou, S., 2020. Post-transcriptional regulation of insect metamorphosis and oogenesis. Cellular and Molecular Life Sciences 77, 1893-1909.

Song, X., Wong, M.D., Kawase, E., Xi, R., Ding, B.C., McCarthy, J.J., Xie, T., 2004. Bmp signals from niche cells directly repress transcription of a differentiation-promoting gene, bag of marbles, in germline stem cells in the Drosophila ovary. Development 131, 1353-1364.
Sreedharan, J., Blair, I.P., Tripathi, V.B., Hu, X., Vance, C., Rogelj, B., Ackerley, S., Durnall, J.C., Williams, K.L., Buratti, E., Baralle, F., de Belleroche, J., Mitchell, J.D., Leigh, P.N., Al-Chalabi, A., Miller, C.C., Nicholson, G., Shaw, C.E., 2008. TDP-43 mutations in familial and sporadic amyotrophic lateral sclerosis. Science 319, 1668-1672.
Sun, J., Deng, W.M., 2005. Notch-dependent downregulation of the homeodomain gene cut is required for the mitotic cycle/endocycle switch and cell differentiation in Drosophila follicle cells. Development 132, 4299-4308.
Weaver, L.N., Drummond-Barbosa, D., 2021. Hormone receptor 4 is required in muscles and distinct ovarian cell types to regulate specific steps of Drosophila oogenesis. Development 148, dev198663.
Weaver, L.N., Ma, T., Drummond-Barbosa, D., 2020. Analysis of Gal4 Expression Patterns in Adult Drosophila Females. G3 (Bethesda) 10, 4147-4158.
Yadav, V., Das, P., Mishra, R., Arya, R., 2022. Cut homeodomain transcription factor is a novel regulator of cortical glia morphogenesis and niche maintenance around neural stem cells. bioRxiv.
Yuan, H., Chiang, C.Y., Cheng, J., Salzmann, V., Yamashita, Y.M., 2012. Regulation of cyclin A localization downstream of Par-1 function is critical for the centrosome orientation checkpoint in Drosophila male germline stem cells. Dev Biol 361, 57-67.

Table S1. Summary of various defects seen in ovaries of 6 days old females of different genotypes examined in this study

Genotype	**Ovary size and fecundity**	**Number of ovarioles**	**Germarium**	**Mid-oogenesis stages**	**Late oogenesis stages**
hsrω^{66} (Figs. 1-4, 7)	Small Low fecundity	Reduced	Region 2b narrower Lower cellular levels of Vasa protein Weaker fusomes with reduced deposition of α-spectrin Hnt expression slightly lower than in wild type Caz expression as in wild type	Enhanced frequency of apoptotic egg chambers Fewer mid stage egg chambers Weak cytoskeleton (F-actin) Cut expression reduced Hnt expression as in wild type Caz expression as in wild type	Fewer post-stage 10 egg chambers but many unovulated mature chambers Weak cytoskeleton Body follicle cell arrangement affected, abnormal dorsal appendages Cut expression lower including in anterior follicle cells at stage 13 Hnt expression as in wild type Caz expression reduced Ovulation block
daGAL4>hsrωRNAi (Fig. 4)	As in wild type Eggs laid	As in wild type	As in wild type	Frequency of apoptotic egg chambers much more enhanced than in *hsrω*^{66}	As in wild type
tjGAL4>hsrωRNAi (Fig. 5)	As in wild type Eggs laid	As in wild type	As in wild type	As in wild type	Mild ovulation block
tjGAL4>EP93D (Fig. 5)	Mostly asymmetric Eggs laid	Reduced	As in wild type	Frequency of apoptotic chambers enhanced as in *hsrω*^{66}	Ovulation block

tjGAL4>UAS-N^{act} (Fig. 5)	Small, No eggs laid	As in wild type	As in wild type	No chambers survive beyond stage 9	No late-stage follicles
tjGAL4>UAS-N^{act}/ hsrω^{66} (Fig. 5)	As in *tjGAL4>UAS-N^{act}* No eggs laid	As in *tjGAL4>UAS-N^{act}*	As in *tjGAL4>UAS-N^{act}*	As in *tjGAL4>UAS-N^{act}*	As in *tjGAL4>UAS-N^{act}*
tjGAL4>UAS-N^{act}/ hsrωRNAi (Fig. 5)	As in *tjGAL4>UAS-N^{act}* No eggs laid	As in *tjGAL4>UAS-N^{act}*	As in *tjGAL4>UAS-N^{act}*	As in *tjGAL4>UAS-N^{act}*	As in *tjGAL4>UAS-N^{act}*
tjGAL4>UAS-N^{act}/ EP93D (Fig. 5)	As in *tjGAL4>UAS-N^{act}* No eggs laid	As in *tjGAL4>UAS-N^{act}*	As in *tjGAL4>UAS-N^{act}*	As in *tjGAL4>UAS-N^{act}*	As in *tjGAL4>UAS-N^{act}*
tjGAL4>cutRNAi (Fig. 6)	As in wild type Eggs laid	As in wild type	As in wild type	Antero-posterior axis length reduced	Small mature follicles with greatly reduced antero-posterior axis length Smaller dorsal appendages Ovulation block
tjGAL4>cutRNAi/hsrω^{66} (Fig. 6)	As in wild type Eggs laid	As in wild type	As in wild type	As in *tjGAL4>UAS-cutRNAi*	As in *tjGAL4> cutRNAi*
tjGAL4>cutRNAi/ hsrωRNAi (Fig. 6)	As in wild type Eggs laid	As in wild type	As in wild type	As in *tjGAL4>UAS-cutRNAi*	As in *tjGAL4> cutRNAi*
tjGAL4>cutRNAi/EP93D (Fig. 6)	As in wild type Eggs laid	As in wild type	As in wild type	As in *tjGAL4>UAS-cutRNAi*	Antero-posterior egg length restored and the ovulation block rescued
tjGAL4>UAS-cut (Fig. 6)	Small No eggs laid	Reduced, and disrupted	Germarium and stage 1-6 egg chambers not identifiable	Only vitellogenic egg chambers with abnormal cellular arrangement	No late-stage or mature egg chambers
tjGAL4>UAS-cut/hsrω^{66} (Fig. 6)	As in *tjGAL4>UAS-cut*	As in *tjGAL4>UAS-cut*	As in *tjGAL4>UAS-cut*	As in *tjGAL4>UAS-cut*	As in *tjGAL4>UAS-cut*

	No eggs laid				
tjGAL4>UAS-cut/ hsrωRNAi (Fig. 6)	As in *tjGAL4>UAS-cut* No eggs laid	As in *tjGAL4>UAS-cut*	As in *tjGAL4>UAS-cut*	As in *tjGAL4>UAS-cut*	As in *tjGAL4>UAS-cut*
tjGAL4>UAS-cut/EP93D (Fig. 6)	Larger than wild type No eggs laid	As in wild type, rescued	As in wild type, rescued	As in wild type, rescued	Late-stage egg chambers undergo apoptosis No mature follicles
tjGAL4>cazRNAi (Fig. 8)	As in wild type Eggs laid	As in wild type	As in wild type although Caz expression absent in follicle cells but highly abundant in germ cells	General oogenesis pattern as in wild type although Caz expression absent in follicle cells but highly abundant in nurse cells and at the posterior end of growing oocyte	Antero-posterior axis length reduced in mature follicles
tjGAL4>cazRNAi/hsrω^{66} (Fig. 8)	As in wild type Eggs laid	As in wild type	As in *tjGAL4> cazRNAi*	As in *tjGAL4> cazRNAi*	As in *tjGAL4> cazRNAi*
tjGAL4>cazRNAi/hsrω RNAi (Fig. 8)	As in wild type Eggs laid	As in wild type	As in *tjGAL4> cazRNAi*	As in *tjGAL4> cazRNAi*	As in *tjGAL4> cazRNAi*
tjGAL4>cazRNAi/EP93D (Fig. 8)	As in wild type Eggs laid	As in wild type	As in wild type	As in wild type	Antero-posterior axis length rescued to normal
tjGAL4>TBPHRNAi (Fig. 8)	As in wild type Eggs laid	As in wild type	As in wild type	As in wild type	Ovulation block
tjGAL4> TBPHRNAi/ hsrωRNAi (Fig. 8)	As in wild type Eggs laid	As in wild type	As in wild type	As in wild type	Ovulation block rescued
ActGAL4>UAS-hsrωRH hsrω^{66} (Fig. 9)	As in wild type Fecundity better than *hsrω^{66}*	As in wild type	As in wild type	As in wild type	Mild ovulation block persists

ActGAL4/ tjGAL4>UAS-hsrωRH hsrω^{66} (Fig. 9)	As in wild type Fecundity better than *hsrω*^{66}	As in wild type	As in wild type	As in wild type	As in wild type Ovulation block completely rescued
20HE fed *hsrω*^{66} flies (examined in 8 days old flies) (Fig. 9)	Not like wild type but better than *hsrω*^{66}, rescued in 80% cases (N=50), Fecundity improved than unfed *hsrω*^{66}	As in *hsrω*^{66}	As in *hsrω*^{66}	Better than *hsrω*^{66}	Better than *hsrω*^{66}, ovulation block rescued in 60% cases